JYVÄSKYLÄ STUDIES IN BIOLOGICAL AND ENVIRONMENTAL SCIENCE
161

Jouni Toivola

Characterization of Viral Nanoparticles and Virus-Like Structures by Using Fluorescence Correlation Spectroscopy (FCS)

JYVÄSKYLÄN YLIOPISTO

JYVÄSKYLÄ STUDIES IN BIOLOGICAL AND ENVIRONMENTAL SCIENCE 161

Jouni Toivola

Characterization of Viral Nanoparticles and Virus-Like Structures by Using Fluorescence Correlation Spectroscopy (FCS)

Esitetään Jyväskylän yliopiston matemaattis-luonnontieteellisen tiedekunnan suostumuksella
julkisesti tarkastettavaksi yliopiston Ambiotica-rakennuksen salissa (YAA303)
toukokuun 5. päivänä 2006 kello 12.

Academic dissertation to be publicly discussed, by permission of
the Faculty of Mathematics and Science of the University of Jyväskylä,
in the Building Ambiotica, Auditorium YAA303,, on May 5, 2006 at 12 o'clock noon.

UNIVERSITY OF JYVÄSKYLÄ

JYVÄSKYLÄ 2006

Characterization of Viral Nanoparticles and Virus-Like Structures by Using Fluorescence Correlation Spectroscopy (FCS)

JYVÄSKYLÄ STUDIES IN BIOLOGICAL AND ENVIRONMENTAL SCIENCE 161

Jouni Toivola

Characterization of Viral Nanoparticles and Virus-Like Structures by Using Fluorescence Correlation Spectroscopy (FCS)

UNIVERSITY OF JYVÄSKYLÄ

JYVÄSKYLÄ 2006

Editors
Jari Haimi
Department of Biological and Environmental Science, University of Jyväskylä
Pekka Olsbo, Marja-Leena Tynkkynen
Publishing Unit, University Library of Jyväskylä

URN:ISBN:9513924041
ISBN 951-39-2404-1 (PDF)

ISBN 951-39-2446-7 (nid.)
ISSN 1456-9701

Jyväskylä University Printing House, Jyväskylä 2006

Tulipa merestä Tursas
Uros aalloista yleni;
Tunki heinäset tulehen,
Ilmivalkean väkehen,
Ne kaikki poroksi poltti,
Kypeniksi kyyätteli;
  Tuli tuhkia läjänen,
Koko kuivia poroja;
Saip' on siihen lemmen lehti
Lemmen lehti, tammen terho,
Josta kasvoi kaunis taimi,
Yleni vihanta virpi,
Nousi maasta mansikkaisna.
  Ojenteli oksiansa,
Levitteli lehviänsä:
Latva täytti taivahalle,
Lehvät ilmoille levisi.
Piätti pilvet juoksemasta,
Hattarat hasertamasta,
Päivän peitti paistamasta,
Kuuhuen kumottamasta.

Ote kirjasta
Kalevala
Runo II
67-88

ABSTRACT

Toivola, Jouni
Characterization of viral nanoparticles and virus-like structures by using fluorescence correlation spectroscopy (FCS)
Jyväskylä: University of Jyväskylä, 2006, 75 p.
(Jyväskylä Studies in Biological and Environmental Science
ISSN 1456-9701; 161)
ISBN 951-39-2404-1
Yhteenveto: Virus-nanopartikkelien sekä virusten kaltaisten rakenteiden tarkastelu fluoresenssikorrelaatio spektroskopialla
Diss.

The movement of viruses can largely be explained by active transport within cellular components, like endosomal vesicles or as diffusion e.g. complexed with antibodies. Fluorescence correlation spectroscopy (FCS) characterizes single molecules and macromolecular interactions both in solution and in living cells. This analytical method uses a laser excitation source and collects traces of single emission fluctuations from a probe volume of subfemtoliter as fluorescent molecules are driven through the sample by stochastic diffusion. The fluctuation carries information about the size, the concentration, and the chemical reactions of the molecules studied. The baculovirus, *Autographa californica* multicapsid nuclear polyhedrovirus (*Ac*MNPV), is an enveloped virus with a physical size of approximately 50 nm X 250 nm and it infects specifically certain lepidopteran species. *Ac*GFPgp64 is a genetically modified version of *Ac*MNPV which has green fluorescent protein (GFP) fused to a major envelope glycoprotein gp64. The results presented in this thesis showed that approximately 4.5 fluorescent units were incorporated in the viral membrane and that the hydrodynamic radius of the virus was 83 ± 19.0 nm. Complexes between human parvovirus B19 virus-like particles (VLPs) and the antibodies present both in acute and past-immunity serum samples gave hydrodynamic radii of 157 ± 151 nm and 69 ± 27 nm, respectively. Cellular localization and diffusion of the recombinant B19 human parvovirus-like particles displaying enhanced green fluorescent protein (EGFP) were described. Finally, the deletions introduced to the amino terminally-truncated canine parvovirus VP2 protein was fused to EGFP. The capability of the truncated VP2 to form capsids was evaluated by monitoring the macromolecular size and the number of the fusion proteins present in fluorescent VLPs. The findings of this thesis gave information about the viral surface composition, viral interactions with antibodies and the diffusion of 1 recombinant enveloped virus and 6 non-enveloped, structurally modified viral nanoparticles.

Key words: Assembly; autocorrelation; baculovirus; fluorescence correlation spectroscopy; green fluorescent protein; parvovirus; recombinant; virus-like particles

Jouni Toivola, University of Jyväskylä, Department of Biological and Environmental Science, P.O. Box 35, FIN-40014 University of Jyväskylä, Finland

Author's address

M.Sc Jouni Toivola
Department of Biological and Environmental Science
University of Jyväskylä
P.O. Box 35
FIN-40014 University of Jyväskylä, Finland
E-mail: jopato@cc.jyu.fi

Supervisors

Dr. Professor Christian Oker-Blom
Department of Biological and Environmental Science
University of Jyväskylä
P.O. Box 35
FIN-40014 University of Jyväskylä, Finland
E-mail: okerblom@cc.jyu.fi

Dr. Professor Matti Vuento
Department of Biological and Environmental Science
University of Jyväskylä
P.O. Box 35
FIN-40014 University of Jyväskylä, Finland
E-mail: vuento@bytl.jyu.fi

Reviewers

Dr. Sarah Butcher
Institute of Biotechnology and Department of Biological and Environmental Science
P.O. Box 65 (Viikinkaari 1)
FI-00014 University of Helsinki, Finland
E-mail: sarah.butcher@helsinki.fi

Dr. Professor Erkki Soini
Faculty of Medicine\Institute of Biomedicine
Biocity, 5th floor, Tykistökatu 5
P.O. Box 123
20521 TURKU
E-mail: erkki.soini@utu.fi

Opponent

Dr. Professor Aladdin Pramanik
Division of Medical Biophysics
Dept. of Medical Biochemistry and Biophysics (MBB)
Karolinska Institute
Scheeles väg 2
S-171 77 Stockholm, SWEDEN
E-mail: aladdin.pramanik@mbb.ki.se

CONTENTS

LIST OF ORIGINAL PUBLICATIONS

This thesis is based on the following scientific articles, which will be referred to in the text by their Roman numerals (I-V).

I Toivola, J., Ojala, K., Michel P. O., Vuento, M., and Oker-Blom, C., 2002. Properties of Baculovirus Particles Displaying GFP Analyzed by Fluorescence Correlation Spectroscopy. Biol. Chem. 2002 Dec; 383 (12):1941-6.

II Toivola, J. Michel, P.O., Gilbert, L., Lahtinen, T., Marjomäki, V., Hedman, K., Vuento, M., and Oker-Blom, C. 2004. Monitoring Human Parvovirus B19 Virus-Like Particles and Antibody Complexes in Solution by Fluorescence Correlation Spectroscopy. Biol. Chem. 2004 Jan; 385, (1):87-93.

III Toivola, J., Gilbert, L., Michel, P., White, D., Vuento, M., and Oker-Blom, C. 2005. Disassembly of Structurally Modified Viral Nanoparticles: Characterization by Fluorescence Correlation Spectroscopy. C. R. Biologies 328 (2005): 1052-1056.

IV Gilbert, L., Toivola, J., White, D., Ihalainen, T., Smith, W., Lindholm L., Vuento, M., and Oker-Blom, C. 2005. Molecular and Structural Characterization of Fluorescent Human B19 Virus-like Particles. Biochem. Biophys. Res. Commun. 2005 23; 331(4):527-535.

V Gilbert, L.[**], Toivola, J.[**], Välilehto, O., Saloniemi, T., Cunningham C., White, D., Vuento M., and Oker-Blom, C. 2006. Truncated Forms of Viral VP2 Proteins Fused to EGFP Assemble into Fluorescent Virus-like Particles (Submitted).

[**] Equal contribution

RESPONSIBILITIES OF JOUNI TOIVOLA IN THE ARTICLES OF THE THESIS

Article I: I am responsible for the study and I also wrote the article.

Article II: I am responsible for the study and I also wrote the article. Patrik Michel did partly his master's thesis in this project.

Article III: I am responsible for the study and I also wrote the article.

Article IV: I am responsible for the FCS analysis and I participated in the writing process of the manuscript.

Article V: Leona Gilbert and I contributed equally to this study and we wrote the article together.

All these studies were carried out under the joint supervision of Professor Matti Vuento and Professor Christian Oker-Blom.

ABBREVIATIONS

aa	amino acid
AAV	adeno associated virus
*Ac*MNPV	*Autographa californica* multicapsid nucleopolyhedrovirus
ADP	Avalanche photo diode
AP	alkaline phosphatase
ARP	autonomously replicating parvovirus
ASD	anomalous subdiffusion
B19	human parvovirus B19
BCIP	5-bromo-4-chloro-3-indolyl phosphate
BPV	bovine parvovirus
BSA	bovine serum albumin
BV	budded virus
C	concentration
CMC	critical micellar concentration
CPV	canine parvovirus
CPM	counts per molecule
CR	count rate
D	diffusion coefficient
DAB	3, 3′-diaminobenzidine tetrahydrochloride
dsDNA	double stranded deoxyribonucleic acid
DTT	dithiotreitol
EGFP	enhanced green fluorescent protein
EIA	enzyme immuno assay
EM	electron microscopy
FCS	fluorescence correlation spectroscopy
FPV	feline panleukopenia virus
GFP	green fluorescent protein
gp64	major envelope glycoprotein 64
GV	granulovirus
HRP	horse radish peroxidase
HTS	high-throughput screening
Ig	immunoglobulin
ITR	internal terminal repeat
K	Boltzmann constant
MEV	mink enteritis virus
mRNA	messenger ribonucleic acid
MVM	minute mice of virus
N	number of molecules
NA	numeric aperture
N_A	Avogadro number
NBT	nitro blue tetrazolium
NPV	nucleopolyhedrovirus

NS	nonstructural protein
ORF	open reading frame
ODV	occlusion-derived virus
ω	omega, radial dimension of confocal volume element
PAGE	polyacrylamide gel electrophoresis
PBS	phosphate-buffered saline
p.i.	post infection
PLA_2	phospholipase A2
PPV	porcine parvovirus
RER	rough endosomal reticulum
Rh6G	Rhodamine 6G
RT	room temperature
SDS	sodium dodecyl sulphate
ssDNA	single stranded deoxyribonucleic acid
SMD	single molecule detection
SNR	signal-to-noise ratio
SP	structural parameter
T	absolute temperature
τ	diffusion time
TMR	tetramethyl Rhodamine
UV	ultraviolet
V	volume
VLP	virus-like particle
VP	viral protein
η	viscosity
r	hydrodynamic radius
Q	quantum yield

1 INTRODUCTION

Small biomolecules, as well as larger macromolecules in living systems follow the laws of thermodynamics, diffusing randomly in solution. Interactions between two physically attractive biomolecules will be followed by a rise in molecular weight. The diffusion properties of such molecules in solution can be studied by using fluorescence correlation spectroscopy (FCS). FCS is a highly sensitive biophysical method for measuring individual molecular characteristics and interactions in solution. In the 1970's physicists formulated the background of the FCS theory and the basic FCS approaches (Ehrenberg & Rigler 1974, Elson & Madge 1974). Applications for biomedical fields were invented, but it took a few decades for the theory and the technology to merge. (Rigler & Elson 2001). Since then, technical advances in single molecule detection (SMD), such as optical improvements, and in photon counting devices like avalanche photo diodes (ADPs), have been significant (Rigler 1995, Rigler et al. 1993). This has enabled monitoring thermal motion of single molecules from volumes of less than one femtoliter. Monitoring dilute solutions has made it possible to analyze conformational fluctuations of single protein molecules (Elson 2001). Lately, the method has been applied to living cells. This includes biological interactions such as binding between a ligand and a receptor directly at the surface of a living cell (Margittai et al. 2003, Pramanik & Rigler 2001, Rigler et al. 1999, van den Berg et al. 2001, Widengren & Rigler 1998) or other rapid complex formations e.g. polymerization of amyloid beta-peptide (Tjernberg et al. 1999), prion aggregates in the cerebrospinal fluid of Alzheimer's patients (Pitschke et al. 1998) or polymerization of fibrin (Bark et al. 1999). The principle of FCS is that the continuous diffusion of fluorescently labeled molecules through the confocal volume element (measuring volume in the order of 0.2 fl) causes fluctuations in the fluorescence intensity (Ehrenberg & Rigler 1974, Ehrenberg & Rigler 1976, Madge et al. 1974). This fluctuation is analyzed using an autocorrelation function. The formed autocorrelation function has two specific characteristics. It contains; 1) indirect information about the size of the molecules studied and 2) information on the concentration of fluorescent molecules present in the confocal volume element. Fluctuation in

fluorescence intensity is related to the time the molecules spend in the confocal volume element, which is also related to the diffusion coefficient (*D*) of the observed molecule. Only the photons emitted by the molecules present in the confocal volume element are detected and registered. In addition to the detected emission, confocal volume element reduces Raman scattering resulting to a significantly improved signal-to-noise ratio. Photophysical properties of the fluorescent molecules have also been studied extensively (Widengren et al. 1995). The fluctuation of fluorescence intensity is also related to the absolute number of fluorescent particles present in the confocal volume element, and thus it is possible to follow changes in very small biological fluid systems, allowing one to measure e.g. how many ligands interact with or dissociate from specific target molecules inside cells (Schwille et al. 1997a). The movement of viral nanoparticles can also be regarded as stochastic diffusion and can be evaluated by FCS (I, II, III, IV, and V).

The aim and the goal of the experimental work in this thesis were to evaluate the diffusion properties of various recombinant viruses and virus-like particles (VLPs) in solution by using FCS. New insights into the structures of the viral nanoparticles and their assemblies were discovered. Viral surfaces were studied by monitoring the number of fusion proteins present on recombinant viral capsids or envelope. An application characterizing antibody-virus interactions for the detection of antibody classes at low target molecule concentration was performed by using FCS.

The review of the literature in this thesis describes a general overview of the FCS and its applications in life sciences. The reader will also be introduced to parvovirus biology as well as to the biology of baculoviruses.

2 REVIEW OF THE LITERATURE

2.1 Fluorescence correlation spectroscopy (FCS)

2.1.1 Background

Fluorescence correlation spectroscopy (FCS) is a spectroscopic method analyzing spontaneous fluctuations of fluorescence as fluorescent molecules diffuse through a confocal volume element of few a femtoliters (10^{-15} L) or less. In the early days of FCS, over 30 years ago when the theory and applications were developed (Elson & Madge 1974), the background noise was very high and it was hard to get reasonable signal-to-noise ratios (SNR). SNR means the ratio of the counts per molecule to the background counts. This problem arose from the fact that the background fluorescence in the method sets the lower detection limit and high fluorophore concentrations had to be used (Widengren & Rigler 1998). However, the possibility of measuring rotational diffusion in a time range much longer than the lifetime of the fluorescence itself, opened up a possibility to measure freely moving labeled molecules in solution (Ehrenberg & Rigler 1974). Continuous research in the field led to reduction of the actual measuring volume followed by substantial improvement in SNR (Rigler et al. 1993). The first improvements with the home-made FCS apparatus allowed the monitoring of molecules down to a particle concentration of C = 10^{-14} M, corresponding to a particle number of 33 in a confocal volume element of V = 5.6 femtoliter (fl) (Rigler & Widengren 1990). Technical improvements were followed by a decrease in the volume element down to 0.2 fl with the release of commercial confocal instruments to the market. The decrease in the actual measuring volume led to a situation where only very few molecules pass the confocal volume element (Auer et al. 1998), allowing monitoring of single particle fluctuations. Thus, during the observation time just one molecule can be excited and detected. Simultaneously, a 40-fold decrease in the background fluorescence signal was obtained, compared to the signal from Rhodamine 6G (Rh6G) alone (Rigler et al. 1993). Collecting photons from the confocal volume

element substantially shortened the retention time of diffusing components (Rigler 1995), and it became possible to use weaker fluorochromes (Widengren et al. 1995). Before the use of diffraction limited confocal excitation, the excitation volume element was too wide and the molecules were exposed too long under the laser beam. Processing random fluctuations from small number of particles at a time with on-line autocorrelations made it possible to use shorter measurement times (Rigler 1995). An analysis for high-throughput screening (HTS) e.g. for drugs and pharmaceutical compounds has been developed (Auer et al. 1998, Eigen & Rigler 1994, Maiti et al. 1997, Rigler 1995). Recently, FCS has also been developed into applications aimed at studying single molecule events in living cells (Issaeva et al. 2004, Pramanik 2004, Pramanik & Widengren 2004).

2.1.2 Principle

FCS characterizes single molecules in solution over many fluorescence intensity fluctuations, collecting photons from the confocal volume element, which is in the order of 1 fl or less (Rigler et al. 1993). The intensity fluctuation collected from the confocal volume element is averaged over time (Fig. 1). Useful information, such as particle size and concentration of particles in the measuring volume can be extracted (Boonen et al. 2000, Henriksson et al. 2001, Maiti et al. 1997, Meyer-Almes & Auer 2000, Rigler 1995, Rigler et al. 1993, van den Berg et al. 2001, Widengren & Rigler 1997) .The fluctuation in fluorescence intensity arises from many sources. It may purely arise from the diffusion of fluorescent molecules in and out of the confocal volume element i.e. by random walk of molecules (Madge et al. 1974), triplet state phenomenon (Widengren et al. 1995, Widengren et al. 1994), concentration-characteristic fluctuations of fluorescence (Widengren & Rigler 1997), or from changes in protein conformation i.e. from conformational fluctuations (Elson 2001, Haupts et al. 1998).

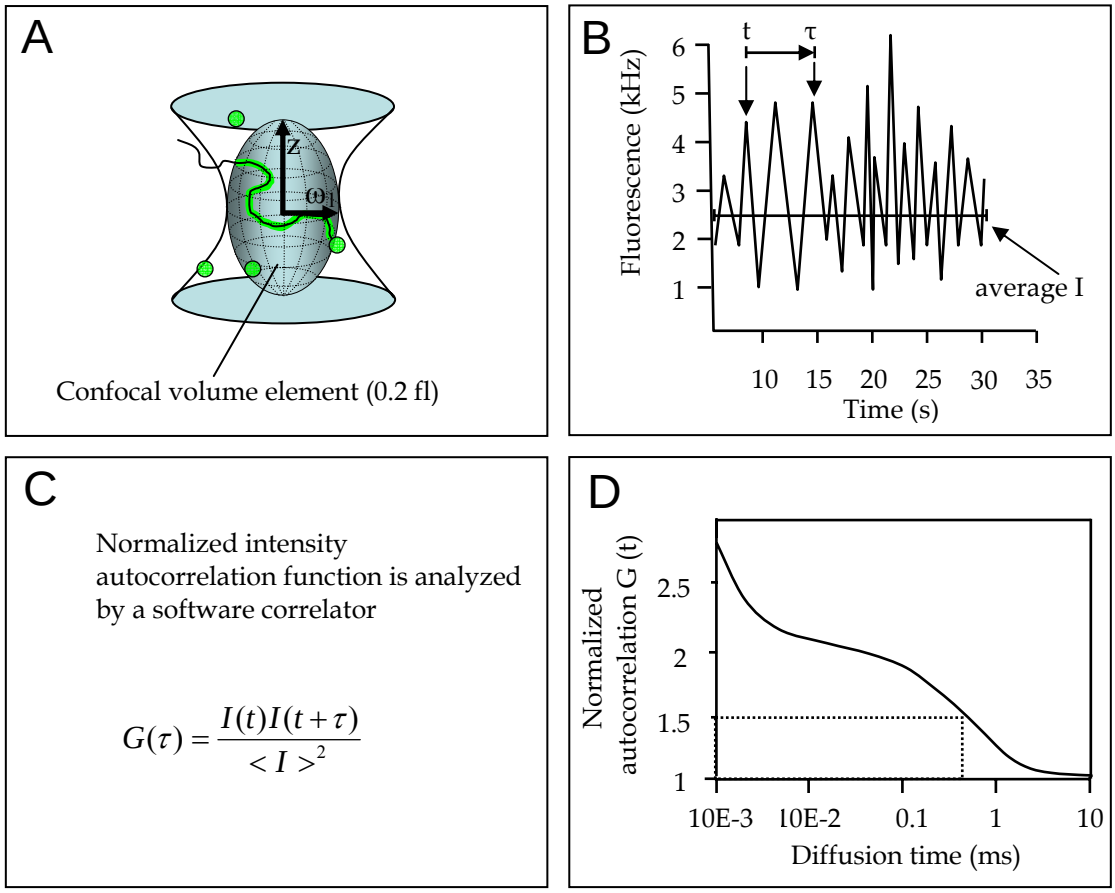

FIGURE 1 Schematic representation of the principle of FCS. Fluorescent molecules (green dots) diffuse through the 0.2 fl confocal volume element, emitting simultaneously photons, which are detected by ADP (green line) (A). ADP collects then the photons, and the fluorescence intensity fluctuations are formed (B) by software correlator (C). Software processes the parameters by an algorithm in the form of an autocorrelation function. The diffusion time of the fluorescent molecule is found from the half decay of the amplitude of the G(t) (D).

When the chemical relaxation time of the detected molecule is much smaller than the diffusion time ($\tau_{chem} << \tau_{diff}$), FCS characterizes pure diffusion (Chattopadhyay et al. 2002, Leng et al. 2002, Rigler et al. 1993, Widengren & Rigler 1997). The chemical relaxation time of molecules is related to the rate where molecules undergo changes in perturbed system towards chemical equilibrium. In contrast, when the chemical reaction does not take place in the time that it takes for a molecule to enter or leave the confocal volume element ($\tau_{chem} >> \tau_{diff}$), dynamic processes are being monitored (Chattopadhyay et al. 2005, Eigen & Rigler 1994, Henriksson et al. 2001, Pramanik et al. 2001). Molecules pass rapidly through the confocal volume element, or remain there longer, depending on the stochastic route and the size of the moving macromolecule. Also, if the bound complex hinders the fluorescence by covering the fluorescent molecules, quenching is seen and less fluorescence is

collected. Both of these phenomena will cause fluorescence intensity fluctuations. A narrow intensity peak in the fluctuation represents small molecules that pass rapidly through the confocal volume element, and in the case of a larger burst, a bigger complex will have passed the laser beam. These bigger particles, in contrast, will diffuse through the confocal volume element slowly, releasing photons by a continuous flux. Thus, smaller fluorescent ligands can be separated from bigger complexes containing the target molecule. Fluctuation in the fluorescence intensity will also be followed when two biomolecules are interacting and forming larger complexes, or aggregates (II, (Lamb et al. 2000) or even when large complexes are formed like e.g. in prion protein multimerization in Alzheimer's disease (Pitschke et al. 1998). Intensity fluctuation has also been autocorrelated directly from cells, where motor proteins at the cellular tubular network-like structures move along the axis of microtubules (Trepagnier et al. 2004). The autocorrelation analysis provides information about the single molecular species (Bacia & Schwille 2003);

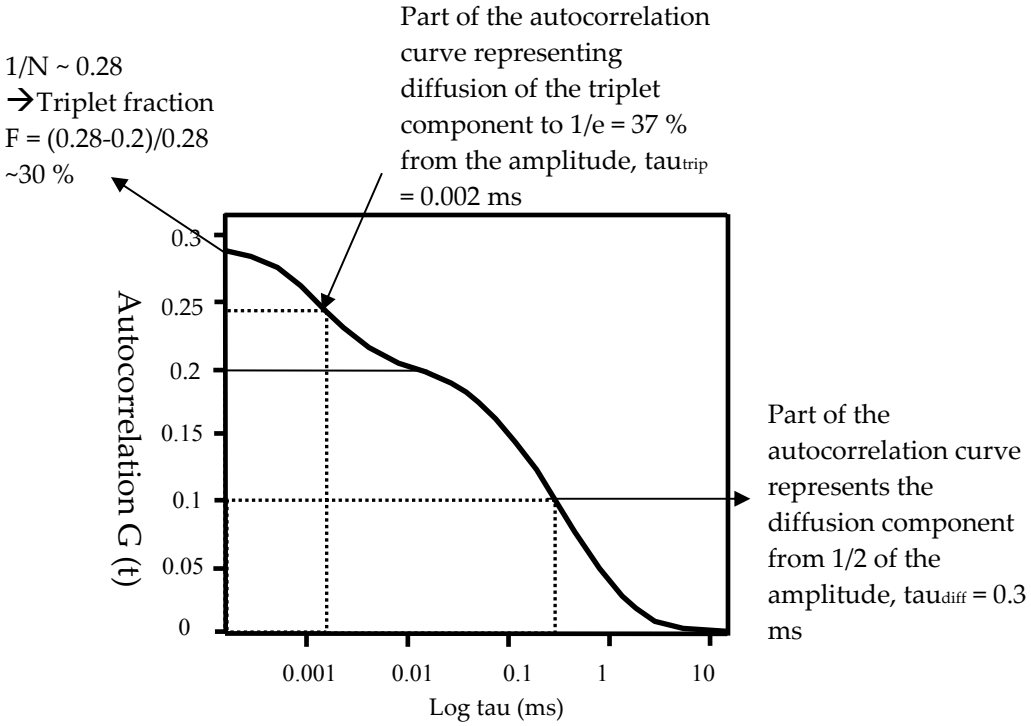

FIGURE 2 An example of an autocorrelation curve. Modified from (Bacia & Schwille 2003).

The autocorrelation curve produced in a statistical manner provides information on the molecular size, derived from the diffusion time. Indirect information on concentration can also be obtained from the amplitude of the autocorrelation function (Gosch & Rigler 2005) (Fig. 2) since the amplitude is inversely proportional to the number of the fluorescent particles present in the confocal volume element. The events in the autocorrelation curve during the first 1-2 μs (Fig. 2) can be regarded as instrumental noise, rotational diffusion of the fluorescent molecules, and as the decay in the triplet state (0.002 ms), which

can be neglected. The translational diffusion time of the molecule of interest can further be monitored from the half decay of the autocorrelation amplitude as can be seen in Figure 2. Well known parameters of autocorrelation measurement can be fixed. Usually these parameters are diffusion time, triplet population, and structural parameter (SP). SP is measured for the correct shape of the confocal volume element and it is defined by the relation of the axial radius and the horizontal radius of the same volume. The diffusion time of the dye molecule is usually 30-50 microseconds (depending on the size of the confocal volume element), the triplet state population should not exceed 20% of total number of fluorescent molecules and the structural parameter is usually fixed to 5. Fixing these parameters using reproducible values will give a good fit after the autocorrelation measurement. The software in FCS uses a special algorithm for calculating the fit (Marquardt 1963). The fit gives a model that indicates how reliable the experiment is with respect to the autocorrelation data obtained. Unwanted complexes, such as aggregates that contribute to the autocorrelation curve, will thus give an unwanted shape to the curve, giving an unsatisfactory fit. Binding to non-specific reacting components may also cause artefacts. The fit will help then to determine whether the bound particles that correlate are specifically those that are being analyzed. Measured diffusion time for the molecule of interest is an average over a large number of fluctuations of molecules (or molecular events such as interactions), before a reliable diffusion coefficient can be calculated (Elson 2001). The diffusion time can then be used to determine the size of the molecule i.e. the hydrodynamic radius. This is described in more detail in section 2.1.3.

2.1.3 Mobility of particles in solution defines the molecular size

The molecules under investigation will have a certain diffusion time, which is the time that takes for a molecule to pass the confocal volume element. The diffusion time of the molecule under FCS confocal volume element is directly related to the diffusion coefficient of the particle, and therefore to the size of the molecule. The shape of the curve measured by the autocorrelation function G (t) allows faster moving particles to be separated from slower ones. The diffusion time doubles, when the size of the molecule increases by a factor of 8. When distinguishing two components in solution, differences in diffusion times have to be greater than the order of 1.6 (Meseth et al. 1999, Trier et al. 1999). All randomized fluctuation data were collected and recorded to form the autocorrelation function G(t) (Gosch & Rigler 2005, Rigler et al. 1998):

$$G(\tau) = 1 + \frac{1}{N}\left(\frac{1}{1+\frac{\tau}{\tau_D^f}}\right)\left(\frac{1}{1+\left(\frac{\omega_1}{z}\right)^2\frac{\tau}{\tau_D^f}}\right)^{\frac{1}{2}} \qquad (1)$$

Here, N denotes the number of fluorescent molecules present in the confocal volume element, τ represents the correlation time, τ_D^f is the mean retention time of the fluorescent particle in the confocal volume element, whereas ω_1 is the horizontal radius, and z the axial radius of the same volume (Fig. 1A). Equation 1 is valid for globular particles, but not for rod-shaped molecules e.g. DNA molecules. The time that it takes for the particle to diffuse through the confocal volume element, $\tau_{diff,}$ is related to the diffusion coefficient D, as well as to the horizontal radius, $\omega_{1,}$ of the laser beam in equation

$$\tau_{diff} = \frac{\omega_1^2}{4D} \tag{2}$$

where ω_1 is used to calculate the confocal volume element and D is the diffusion coefficient of the molecule under study. The diffusion time for the molecule of interest is measured and this can be used to determine the diffusion coefficient D for a molecule (Wilk et al. 2004) under measurement, from the ratio of $D = D_{Rh6G} \cdot \tau_{Rh6G} / \tau_{sample}$. D can be then used for several purposes, such as a tool for measuring association kinetics (Boonen et al. 2000, Meyer-Almes et al. 1998) in cellular environments (Meissner & Haberlein 2003) or in determining the physical size of a macromolecule. Since ω_1 is known, it is possible to measure the diffusion time of the molecule through the confocal volume element (Rigler & Widengren 1990). Measured SP (structural parameter) of the fit is used for calculation of the confocal volume element. For a well adjusted pinhole of the instrument, SP is 5. The structural parameter is the ratio of ω and z in Eq. 1. Since the particle mobility through the confocal volume element is obtained, the hydrodynamic radius for globular particles can be calculated by using Stokes-Einstein relation as follows;

$$D = \frac{kT}{6\pi r \eta} \tag{3}$$

This important equation takes into account the viscosity and the temperature of the solution. In the equation (3) k is the Boltzmann constant, T is the absolute temperature, r the radius of the particle, and η is the viscosity. Both viscosity and temperature will affect the diffusion time. Therefore, the measurement system should always be thermostated to avoid differences in temperature that would result in a change in the calculated radius of the particle.

2.1.4 Number of molecules in solution

Table I shows the relation of particle number and the concentration in confocal the volume element. When the number of molecules (N) is less than 0.5 molecules at a time in the confocal volume element, concentrations below nanomole/litre is achieved (Table 1).

TABLE 1 Concentrations in confocal volumes in ConfoCorII, in [nM]. Table is modified from application manual (Zeiss 2001). *N* is the number of molecules present in the confocal volume element of 0.38 fl from the confocal volume element of 488nm laser beam.

N	[nM]
0.1	0.44
0.2	0.87
0.5	2.2
1.0	4.4
2.0	8.7
5.0	22.4
10	43.6

The more fluorescent ligands are present in the confocal volume element, the lower is the amplitude of the autocorrelation, i.e. the amplitude is inversely proportional to the particle number, and thus it is possible to monitor local concentration fluctuations (Schwille et al. 1997a). The sensitivity of the method can thus be applied to ligand-receptor analysis at cell surfaces or monitoring other dynamic events inside the cells (Bacia & Schwille 2003) where low concentration of target molecules are present. Molecules present on the cell surfaces even below concentrations of one macromolecule per square micrometer can be monitored (Maiti et al. 1997) and it is possible to measure kinetics below nanomolar concentrations (Jermutus et al. 2002, Rigler 1995). In some cases when association takes place at a ligand concentration much higher than the upper detection limit of the method (200 nM), a large amount of fluorescent ligand is required. This will be followed by a decrease in the SNR and thus will lower the sensitivity (Rigler 1995), making it harder to measure binding constants for those molecules that require high amounts of ligands for association. In the lower range of the concentration, in contrast, too rare emission bursts are harder to correlate (Bacia et al. 2002) and the noise becomes equal to the signal (Rigler & Widengren 1990). For reasonable SNR it would be preferential that the counts per molecule (CPM) should exceed the basic level of the count rate. This means that a low particle number of fluorescent molecules with efficient quantum yield (Q) (Schwille & Kettling 2001) should be used in a confocal volume element (Bacia et al. 2002). Quantum yield describes the ratio of fluorescence intensity to the excitation intensity, Qe/Qex, where e is emission, and ex is excitation. With reasonable quantum yield the autocorrelation curve represents better single fluctuation of molecules with higher autocorrelation amplitude. However, as the particle number increases, information at the single molecule level is lost when the relative fluctuation decreases (Rigler & Widengren 1990). When monitoring single molecule fluctuation by FCS, the criteria of less than one molecule at the time in the confocal volume element would be ideal. This means particle number of 0.2-0.5. Interactions can be monitored directly in a concentration dependent manner using the amplitude of the autocorrelation curve. Even 0.1 particles in the

confocal volume element will give SNR good enough for FCS measurement (Schwille et al. 1997a). The concentration of fluorescent molecules can be calculated by using the following formula:

$$C = \frac{N}{N_A \cdot V} \qquad (4)$$

Here, N_A is the Avogadro's number with 6.022×10^{23} mol^{-1}, N is the number of particles per confocal volume element and V is the volume size of the confocal volume element (Foldes-Papp et al. 2001b, Foldes-Papp et al. 2002). The same equation can also be expressed as

$$C = \frac{\left(\frac{N}{0.25\,fl}\right) \cdot 10^{15}}{N_A} \text{ (I, II).}$$

2.1.5 Kinetic associations measured by FCS

The particle radius derived from the measured diffusion time can also be useful when comparing the differences in size between fluorescent components in the solution. Decrease in the number of fluorescent ligand per confocal volume element is followed by a shift in the autocorrelation curve to the right (Henriksson et al. 2001, Pramanik et al. 2001). The shift reflects the ongoing complex formation among the components used in the equilibrium mixture. Measuring particle populations can thereby be useful when specific binding constants are studied. Binding constants have been measured, with labeled ligands at cell surfaces (Pramanik et al. 2001, Pramanik & Rigler 2001), with specific peptides (Boldicke et al. 2000, Henriksson et al. 2001), DNA-enzyme complexes (Auer et al. 1998) and receptor-ligand complexes (Meissner & Haberlein 2003, Rauer et al. 1996). After binding, by using an excess of non-labeled ligand (usually 1000-fold excess), the dissociation time (Tau_{diss}) for a molecule can thereby be calculated (Henriksson et al. 2001). From the previously measured titration experiments, K_{ass} –value can further be obtained, and by using this value, by calculating $1/Tau_{diss}$, the dissociation constant (K_{diss}) is obtained from half of the amount of fluorescent ligands in complex.

2.1.6 Diffusion properties of molecules in solution

The diffusion of molecules present in solution depends on a number of factors. Namely, they are the molecular mass of the particle (m), temperature (T) and the viscosity (η) of the solution (Eq. 3). The more viscous the sample solution is, the slower is the movement of the particle. In contrast, when more heat is brought to the system, the thermal movement of the particles becomes more vigorous due to increase in enthalpy. Therefore, the parameters T and η should always be standardized prior to analysis.

2.1.7 FCS in cell biology

Many biological processes inside cells begin from small molecular nanostructures such as nucleotides, amino acids or lipids that can form larger structures like DNA, proteins or membranes, respectively. One example of complex formation is transcription initiation complex forming prior to gene transcription. The formation of this kind of molecular clusters can be monitored by FCS. In the future, the method will probably be used more in developing novel drugs for pharmaceutical use. FCS as a tool in HTS (High Throughput Screening) (Eigen & Rigler 1994) creates a possibility to screen thousands of possible interactions between fluorescently labeled ligands (drugs, peptides) and biological macromolecules (receptors, enzymes, active sites in DNA). Those selected molecules carry the highest or most suitable affinity for biological function. However, using FCS to screen thousands of molecules is principally a question of technical improvements such as faster screening time and sample number (Kask et al. 2000). One major use of FCS is in cell biology. Substancial improvements for utilizing FCS when studying living cells have been developed (Reznikov et al. 2000, Yakovleva et al. 2001, Yakovleva et al. 2002). By introducing a confocal volume element inside the cellular compartments, there is an infinite number of possibilities that can be studied; protein interactions, receptor densities, specific ligands or lipids (Foldes-Papp et al. 2001a, Foldes-Papp & Rigler 2001, Foquet et al. 2002, Pramanik & Rigler 2001). Recently, specific interactions between cell surface proteins and ligands have been studied extensively by using FCS (Pramanik 2004, Pramanik et al. 2001, Rigler et al. 1999, Vukojevic et al. 2004).

Foreign components that do not belong to the cells own machinery can also be studied, e.g. the assembly of viruses (I, III-VI). With FCS, it is possible to monitor freely moving virus particles by their diffusion coefficients D in vitro. When the diffusion coefficient of the virus has been determined, this information can perhaps later be used to monitor viral trafficking in living cells, although such studies with intact viral particles has not yet been performed by FCS. Thus, FCS could be applied to studying viral entry mechanisms and transport through the plasma membrane to the nucleus, and in monitoring viral behavior in their natural environment.

Quantitative information from particle number, as well as the true size, can be analyzed by FCS (VI, I). Ligand concentration sets the limits in FCS since the concentration of the fluorophore should be in the range of 500 pM to 200 nM. Thereby, in order to e.g. measure binding constants, the association range should be between these limits. One interest in the field of biology is to apply FCS for biotechnical and biomedical purposes. Antibodies have previously been used in single molecule detection (Hegener et al. 2002). It is also possible to measure interactions directly between serum antibodies and VLPs (II). As a diagnostic tool, this method could have potential in detecting viruses in low concentration (Eigen & Rigler 1994) (down to nM range). Characterization of enveloped viruses, such as baculoviruses displaying a fusion protein may have potential in measuring large viruses and give information on individual protein

molecules (I). Measuring particles in physiological solution conditions confirms that these biomolecules are intact, and possess their natural conformation (e.g. proteins). The other advantage of this method is that biological interactions are monitored "on-line". Complex systems inside the cells, like large soluble macromolecules are driven by an anomalous diffusion (Masuda et al. 2005), which sets limitations for proper monitoring of diffusion characteristics and dynamics. The effect of anomalous subdiffusion (ASD) has been studied by FCS in several reports (Bacia & Schwille 2003, Masuda et al. 2005, Schwille et al. 1999b, Wachsmuth et al. 2000). Measuring particles or interactions inside the cells may lead to several difficulties since the cellular environment is a complex "network" of fibrils, membranes, cytoplasm, and large macromolecular entities such as RER (rough endosomal reticulum) and ribosomes. On the other hand, mechanical fluctuations nearby the membrane inside the cells can modify the geometry of the confocal volume element and correspondingly change the number of particles (Fradin et al. 2003). Thus, it is hard to detect and extract information from the intracellular diffusion even with FCS (Schwille et al. 1999a, Schwille et al. 1999b). Nevertheless, it is fairly questionable that the diffusion at least for large complexes inside the cells would be anomalous at all, since it is well known that macromolecules either are bound or not bound. An example of this is canine parvovirus, which gains entry to its host cell using clathrin-mediated endocytosis (Parker & Parrish 2000) and escapes from endocytic recycling vesicles possibly via late endosomes (Suikkanen et al. 2002) to the cytosol in order to be transported towards the nucleus for replication (Suikkanen et al. 2003a). Nuclear transport of CPV requires the movement of viral particles along e.g. microtubules (Suikkanen et al. 2002) and cannot, thus, directly be expressed by random diffusion.

In living cells, the signal from autofluorescent molecules has to be below the signal obtained from the detected molecules (Brock & Jovin 1998). When studied from solution, this problem does not exist, since molecular ensembles of the fluorescent species can be diluted down to C = 10^{-14} M. In order to distinguish two different components by the FCS analysis, the difference between the molecular weights of the molecules has to be at least 6-fold, or the diffusion time 1.6 –fold (Meseth et al. 1999, Trier et al. 1999). This means that the size of the molecules in the confocal volume element contributes significantly to the autocorrelation curve. Cross-correlation analysis, however, can distinguish interactions of same sized molecules, since the fluorescence intensity is correlated only for those molecules passing together through the confocal volume element. Cross-correlation is formed from the emissions collected with two channels, one of far red, and one of green, and only the bound ones will give cross-correlation (Schwille & Kettling 2001, Schwille et al. 1997b). Thus, in the cross-correlation mode, the microscope is capable of detecting a simultaneous presence of two different fluorescent labels in the same molecule. Emission wavelengths of the two molecules are separated largely by Stokes shift, and thus there is no overlapping in the fluorescence intensity. Usually wavelengths of 488 nm and 633 nm are used to avoid

overlapping. It is also worth noticing that when two labeled molecules move together by Brownian motion, they in fact are bound to each other.

2.2 Viruses

The movement of macromolecules and other larger particles such as viruses in solution, is random and spontaneous and can be described by Brownian motion (Bouchaud & Georges 1990, Masuda et al. 2005, Saxton 1996). The diffusion characteristics of viruses are not well-known, and FCS has previously been directed only into viral DNA-level studies in protein-DNA or protein-protein complexes (Busschots et al. 2005, Maertens et al. 2005, Oehlenschlager et al. 1996, Vercammen et al. 2002, Weiner et al. 2000) or viral DNA/RNA hybridization (Schwille et al. 1997a). Only a few FCS reports have addressed viral particles alone (Bernacchi et al. 2004) (I-V). Virions are well suitable for FCS, since most of the known viruses are close to the size range (20 nm - 300 nm) of the FCS measuring volume (200 nm X 1500 nm). This allows monitoring of viruses as single particles or as single "macromolecules". Viruses direct the host cellular regulatory system and machinery to produce enzymes required for replication, and in many cases the viral genome encodes proteins, which act e.g as RNA-polymerases, transcriptases needed in replication. Viruses will also use host cell ribosomes to translate viral proteins. Due to this reason, viruses are totally dependent on their host cell survival and therefore they can be regarded as being inert biochemical complexes. Thus, viruses make an exception to what is understood as a concept "life". Viruses carry the genetic material packed tightly inside the viral capsid, in a form of nucleic acids, either DNA or RNA. The genome is covered by an outer shell, which mainly protects virus from physical, chemical or enzymatic damage. The protected nucleic acid encodes those proteins that are essential for viral replication, assembly and release from the host cell to surroundings.

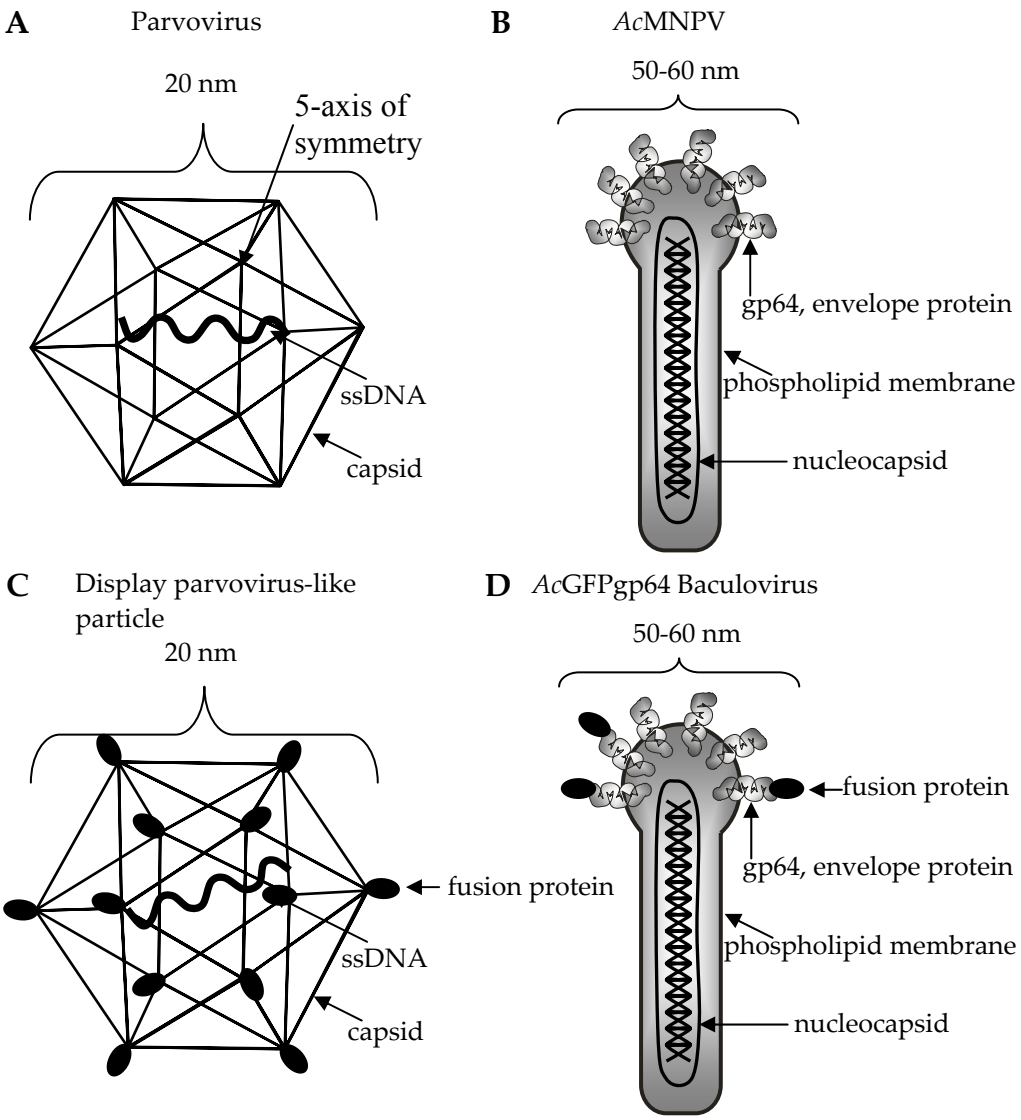

FIGURE 3 Schematic representation of the icosahedral structure of parvoviruses CPV and B19 (A) and a baculovirus, *Autographa californica* (*Ac*MNPV) (B), fusion protein –displaying virus-like particle (C) and baculovirus displaying a GFP-gp64 fusion protein (D). Icosahedrons were drawn by Jouni Toivola, and *Ac*MNPVs are drawn by Jouni Toivola and Anna Mäkelä.

2.3 Baculoviruses

Baculoviridae is a family of rod-shaped viruses with a large double-stranded DNA genome (Fig. 3). These viruses infect specifically insect species as their natural hosts - the strains of these viruses do not propagate in any non-invertebrates. The family is divided into two genera, *Nucleopolyhedroviruses* (NPV) and *Granuloviruses* (GV), which basically are distinguished by the morphology variations in the occlusion bodies (Volkman 1997). The genome is

replicated and transcribed in the nucleus of the infected host cell, where the large DNA is packaged into nucleocapsids. Since the size of this nucleocapsid of the virus is highly variable, baculovirus particles can hold large amounts of foreign DNA; from 80 up to 200 kb (Burgess 1977).

2.3.1 Life cycle of baculovirus

The life cycle of baculoviruses is biphasic and is divided to an early phase, where occlusion-derived viruses (ODVs) are produced and a late phase, where budded viruses (BVs) are produced. The role of BVs is in cell-to-cell infection, whereas ODVs are responsible of spreading the infection from insect to insect. BVs and ODVs both have characteristic envelopes, of which the phospholipid composition is slightly different due their different origins. BVs get the envelope from the insect cell membrane, whereas ODVs get their outer layer from the nucleus. BVs have phophatidylserine as the major envelope component and ODVs, on the other hand, have phosphatidylethanolamine and phosphatidylethanolcholine. These two phospholipids are also major constituents of *Sf*9 insect cells (Marheineke et al. 1998), where baculoviruses are produced. ODVs are enclosed in a protective matrix composed of a large polyhedrin coat, polyhedron (Fig. 4). After lepidopteran larvae have eaten plant leaves naturally contaminated by viruses from infected larvae, the ODVs packed in the polyhedra (Washburn et al. 1999) are released into the insect midgut in the alkaline conditions of the intestine pH (>10) (Blissard & Rohrmann 1990), where the polyhedrin coat is broken down (Blissard 1996, Volkman 1997). The released ODVs fuse directly with cell membranes of microvilli epithelial cells in the intestine of the larvae (Blissard & Rohrmann 1990, Summers & Smith 1987, Washburn et al. 1999). Since enveloped baculoviruses have a lipid-bilayer as an outer shell, they must use different strategies compared to non-enveloped viruses, to enter the cell. Enveloped viruses use outer spike glycoproteins that serve as recognition sites to receptors (Smith & Helenius 2004). Often these glycoproteins have other functions, such as capability to act as membrane fusion factors. The membrane glycoprotein 64 (gp64) of the budded form of *Ac*MNPV mediates endocytosis in to the host cell. Gp64 plays an essential role in the viral infection cycle. It anchors baculovirus to the target cell surface (Hefferon et al. 1999, Ojala et al. 2004), that is why gp64 is also called an envelope-fusion protein (Liang et al. 2005). Although it is known that the virus uses gp64 for anchoring, the target receptor for binding has not been described yet. In addition to binding to the host cell membrane, gp64 takes part in the budding process of forming BVs in the late phase of the infection (Oomens & Blissard 1999). The late phase of infection includes the transportation of nucleocapsids into the nucleus. Baculovirus occlusions produce predominantly large amounts of the single protein, polyhedrin (Rohrmann 1986, Summers & Smith 1978) which can further be taken into account when engineering heterologous proteins for use in baculovirus mediated protein expression.

2.3.2 Baculovirus proteins

The *Ac*MNPV genome is very large and complex. Although the genome has been completely sequenced, the functions of the majority of identified 70 genes still remain unknown. The genome codes for the major envelope glycoprotein gp64, which is known to be the only protein specific to BV envelope. The nucleocapsid of *Ac*MNPV proteins is composed mainly of vp39. The structural protein VP1054 is also required for nucleocapsid assembly (Olszewski & Miller 1997). P24 is associated with nucleocapsids of budded and polyhedrin-derived virions. P74-protein directs specific binding of *Ac*MNPV occlusion-derived virus to targets in the midgut epithelial cells of *Heliothis virescens* larvae (Haas-Stapleton et al. 2004). EGT is a viral product that affects the hormonal regulation of the insect; it increases the ecdysteroid UDP-glucosyltransferase level in insect cells prolonging the larval stage of the insect, instead of turning to pupa (Flipsen et al. 1995). This is an advantage for the virus, increasing its productivity and the number of virions produced. Immediate early expression factors (IEs) have their own role, in gene regulation. Namely, it has been shown, that the "late genes" of *Ac*MNPV are activated by immediate early proteins IE0, with the interaction aid by IE1. Using transient assays, complex activation of very late gene expression from the polyhedrin promoter has been described (Huijskens et al. 2004). Late expression factors (LEFs) also have a role in the regulation and expression of late genes. LEF-10 is thought to be a late expressed structural protein although its exact function is still not known. LEF3 proteins are necessary for the virus to express late genes such as p10 and polyhedrin. Together with helicase p143, LEF3 is needed for viral replication. The function of the LEF -gene family is poorly understood, although it is known that LEF-11 is required for viral DNA-replication during the infection cycle. Additionally, protein pp31 binds to DNA serving as a late expression factor.

2.3.3 Use of baculoviruses in biotechnology

The amount of polyhedrin produced by baculovirus corresponds to a yield of 10-100 mg protein per 10^9 cells. By replacing the original polyhedrin gene, and introducing the foreign gene of interest, large amounts of pure, correctly post-translationally modified protein can be obtained (Miller 1988). The polyhedrin coat is needed for wild-type baculoviruses against environmental stresses such as changes in osmolarity or pH. However, the replacement of the polyhedrin gene is possible, since the gene is not essential for the normal life cycle of the virus in cell culture. Baculovirus nucleocapsids are predicted to have the capacity to handle inserts as large as 100 kb. However, the upper limit for the insert size remains still unknown. Under the control of several promoters, a number of genetically modified transfer vectors simultaneously expressing multiple genes has been generated (O'Reilly et al. 1992). Effective production using baculovirus as an expression vehicle, BEVS (baculovirus expression vector system) has been developed. This is possible under the control of various

promoters acting in cell cultures (Roy 1996), originally isolated from e.g. insect *Spodoptera frugiperda* larvae (*Sf*9 cells).

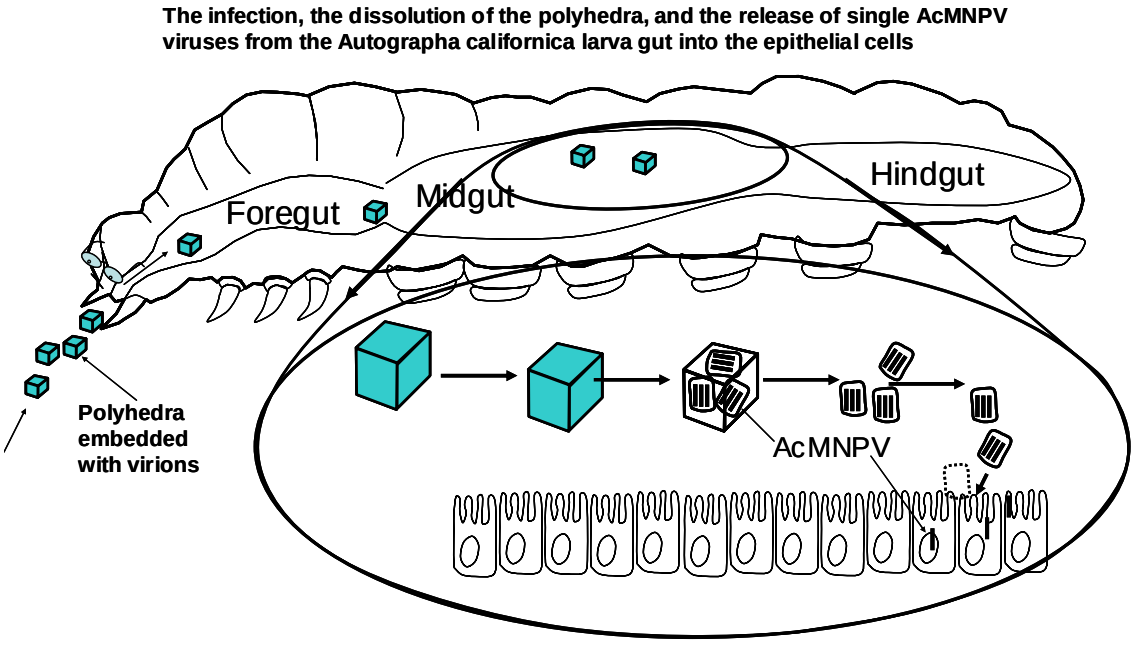

FIGURE 4 *Ac*MNPV is released to the gut epithelial cells, where the infection occurs. The figure is adapted from Frisen and Miller (Friesen & Miller 2001).

Insertion of a foreign gene under the control of appropriate promoters and regulatory elements does not necessarily mean that the expressed recombinant product is correctly post-translationally modified. For instance, it is extremely important in clinical trials, that functional therapeutic proteins have sialic acid moieties at the end of the modified carbohydrate structure (Kost et al. 2005, Marchal et al. 2001). To produce *N*-glycan processing activities absent from the original *Sf*9 –cells, stable transformations to the insect cell lines has been generated. These cell lines were modified in a way, that they are capable of making post-translational modifications typical for mammalian cell lines, such as terminal β-galactosylation of *N*-glycans (Hollister et al. 1998) and sialic acid processing activity (Hollister et al. 2003, Hollister & Jarvis 2001). In addition, insect cells can perform other relevant post-translational modifications, such as proteolytic cleavage, acylation and phosphorylation, which makes it easy and safe to use these cells for production of authentic recombinant proteins.

2.3.4 Baculovirus display

Baculovirus has been shown to be a valuable tool in transducing several mammalian cell lines. Prior to transduction, baculovirus uses the transmembrane glycoprotein gp64 for anchoring to the host cell membrane. A specific transmembrane region and a signal sequence of gp64 have been utilized for targeting baculovirus efficiently to cell membrane. Antigen presentation of whole viral proteins at the baculoviral surface has been successful (Tami et al. 2000). The method has also been used in production of e.g. monoclonal

antibodies when the immunogen is fused to gp64 and the whole recombinant baculovirus is used for immunization (Lindley et al. 2000). A similar kind of baculovirus mediated vaccination was successfully performed when the foreign surface antigen p67 of the protozoan parasite *Theileria parva* was fused to gp64 (Kaba et al. 2003). A virus with a large genetic complexity such as baculovirus can also be used in targeting to mammalian cells e.g. for gene delivery applications. Then it is of importance to develop a display virus where the viral surface protein provides a signal for specific targeting to the tissue of choice. An example of baculovirus gene transfer is where high levels of the transduced foreign gene was expressed in mammalian hepatocytes using baculovirus (Boyce & Bucher 1996). Such gene transfer like this could be used in genetic manipulation of mammalian cells, since baculovirus propagates only in insect cells. Local, stable transformations can be achieved, when the virus transiently transduces malignant cells. Short peptides have been expressed successfully on the surface of baculovirus for targeting purposes. An integrin specific motif, RKK, has been fused to the gp64 protein to mediate specific binding of the virus to a peptide in the alpha2I-domain of alpha2 integrin (Riikonen et al. 2005). Additionally, a small HIV gp41 protein -sequence harboring a few amino acids was presented on the membrane of *Ac*MNPV by insertion in to the gp64 sequence (Ernst et al. 2000). The major capsid protein, vp39, of *Ac*MNPV has also been utilized, when displaying foreign proteins in the viral nucleocapsid. EGFP was successfully fused either to the N- or C- terminus of the vp39 protein resulting in modified vp39 chimeras capable of forming capsids (Kukkonen et al. 2003, Oker-Blom et al. 2003).

2.4 Parvoviridae

Parvoviruses (*Parvoviridae)* with two subfamilies (*Parvovirinae* and *Densovirinae*) are nonenveloped, icosahedral and small viruses with a corresponding molecular mass of 5.5-6.2 X 10^6 Da (Cotmore & Tattersall 1987, Siegel et al. 1985, Tsao et al. 1991). The subfamily *Parvovirinae* is further divided to three main genera. The *Parvovirus* genus belongs to autonomously replicating parvoviruses (ARPs) consisting of 8 distinctive viruses; CPV (canine parvovirus), FPV (feline parvovirus), H1 (H-1 virus), LuIII (LuIII parvovirus), MEV (mink enteritis virus), MVM (minute virus of mice), BPV (bovine parvovirus), and porcine parvovirus (PPV). The genus *Dependovirus,* which is better known as adeno associated viruses (AAVs), serotypes 1-8 is dependent on a helper virus. They differ in their genome as well as in their life cycle, compared to other *Parvovirinae*. Only one member belonging to the *Erythrovirus* genus, human parvovirus B19, is known today. CPV is known to be pathogenic to several carnivore species. Although CPV infects mainly dogs and has a significantly high sequence homology with other autonomous parvoviruses such as FPV and MEV (98 %) (Truyen et al. 1994), they can reliably be distinguished by

monoclonal antibodies (Parrish et al. 1982) or by hemagglutination assays. The capsid structure itself determines the host range variability in many autonomous parvoviruses including porcine parvovirus (Bergeron et al. 1996), MVM (Ball-Goodrich et al. 1991, Gardiner & Tattersall 1988), FPV and MEV (Horiuchi et al. 1992, Parrish 1991). CPV, however, has a more extended host range than FPV, infecting both dogs and cats, while FPV has only the cat as a host (Parker & Parrish 1997). Autonomous parvoviruses are very similar in their life forms and resemble each other both structurally and genetically (Corsini et al. 1995) although having specific host ranges.

AAV's life cycle is biphasic. In the presence of a helper virus they undergo a productive and lytic infection cycle, or instead, if no helper virus is present, they will silence their productivity simultaneously by taking advantage of the site-specific genomic integration to chromosome 19 of the host DNA in order to establish a latent form of virion (Meneses et al. 2000).

Human parvovirus B19, discovered in 1975, (Cossart et al. 1975) is so far the only parvovirus known to be harmful to humans (Katta 2002, Vafaie & Schwartz 2004, Young 1995). In order to be able to infect and replicate in the target cell, this virus needs to bind to P antigens (globoside) at the cell surface of human erythroid progenitor cells (Brown et al. 1993). This is why B19 viremia is described to influence on red blood cell progenitor cells, causing symptoms with aplastic crises in sickle cell anemia and other hemolytic anemias (Frickhofen & Young 1989). B19 has also shown to be responsible for spontaneous abortion in pregnant women due to infection of the fetus (Maeda et al. 1988, Rodis et al. 1988). The virus is also responsible for several other symptoms. Acute phase infection can result in erythema infectosum (fifth disease) occurring in small children (Anderson et al. 1985, Kawase et al. 1995, Pamidi et al. 2000) and transient aplastic crisis for patients under hemolysis (Kawase et al. 1995). When prolonged, the disease can result in severe chronic arthritis (Anderson et al. 1984, Cassinotti et al. 1998, Moore 2000, Takahashi et al. 1998). B19 has also been associated in clinical manifestations such as hepatitis (Naides et al. 1996, Pardi et al. 1998) and myocarditis (Brown et al. 1994).

2.4.1 Parvovirus genome and proteins

In all parvoviruses, the size of the genome is approximately 5 kb, containing short palindromic sequences capable of making hairpin loops (Cotmore & Tattersall 1992). The genome of parvoviruses is composed of single stranded DNA usually of negative polarity (Myers & Carter 1980, Richards et al. 1977, Yuan & Parrish 2001). AAVs, however, can alternatively pack the genome with both negative and positive polarities (Berns & Adler 1972, Cotmore & Tattersall 1987). Replacing LuIII right end origin from original negative MVM strand produced a chimeric strand that contained both polarities (Cotmore & Tattersall 2005). Further, B19 (Agbandje et al. 1991, Cotmore & Tattersall 1984, Shade et al. 1986, Summers et al. 1983), LuIII and BPV can encapsulate genomes of both positive and negative polarities (Astell et al. 1983, Pintel et al. 1983). In autonomously replicating viruses (ARPs) the genome is organized with

palindromic termini at both ends serving as origins of replication (Cotmore et al. 1989). The ARP genome is divided into two open reading frames (ORFs) with different functions. Most ARPs are of negative polarity (3'->5'). The left hand (5') ORF of the genome codes for the non-structural proteins NS1 and NS2 (Cotmore & Tattersall 1987) for which the transcription is mediated by promoter p4. NS1 and NS2 are 83 and 22 kDa proteins, respectively. They both act mainly as factors responsible for inducing cellular cytotoxicity after infection, but NS1 seems to be more effective (Legrand et al. 1993). The NS1 protein also has cellular regulatory functions in viral replication e.g. having both DNA nicking and helicase activities. NS1 has also DNA-binding activity functions (Rhode 1985b) and is required for normal viral replicative forms (Berns et al. 1988, Hermonat et al. 1984, Senapathy et al. 1984). NS1 and NS2 have similar functions both within dependoviruses and ARPs (Rhode 1989). NS1 is also required for transcription of viral proteins VP1 and VP2 (Rhode & Richard 1987, Tratschin et al. 1986). The right hand (3') ORF promoter, p38, is regulated by trans-activation of NS1 (Cotmore & Tattersall 1986, Cotmore & Tattersall 1987). This ORF codes for the structural proteins VP1 and VP2, the proteins responsible for capsid construction and viral entry (Fig 5). VP3 is produced proteolytically from VP2.

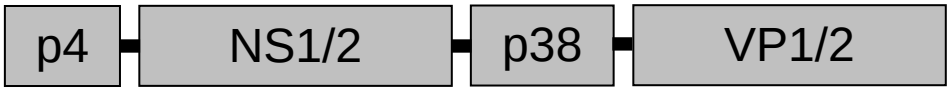

FIGURE 5 Simple representation of the genomic organization of CPV. Negative stranded CPV ssDNA is in 3'-5' orientation. p denotes for promoter, NS for non-structural, and VP for viral protein.

Among different parvoviruses, these three viral proteins VP1, VP2 and VP3 have alternative functions. All capsid proteins share a common β-barrel structure. However, relatively little is still known about capsid assembly of the autonomous parvoviruses, but it is known that two or three viral proteins (VP1-VP3) participate in this event (Yuan & Parrish 2001). Parvoviruses are composed of 60 copies of a combination of viral proteins VP1, VP2 and VP3, and for most of the autonomous parvoviruses VP2 with a molecular mass of 64-66 kDa is predominant (Cotmore & Tattersall 1987, Rose et al. 1971, Tattersall et al. 1976, Tattersall et al. 1977, Yuan & Parrish 2001). The size of VP1 is 83 to 86 kD. In wild-type CPV, VP1 is present to a minor extent (< 10 %), but in B19, the amount is even smaller, ≤ 5 %. In CPV, both VP1 and VP2 are products of alternative splicing from the same primary transcript, and VP2 is included in the whole sequence of VP1, which contains additional aminoterminal residues that are essentially related to viral infectivity. For normal assembly of CPV, both VP1 and VP2, however, are required (Rhode 1985a). Instead, VP3 proteins are present in small proportions in full capsids (capsid that contains DNA). In VP3, there are only 15-20 amino acids missing from the original amino terminal sequence of VP2 (Tsao et al. 1991). Interestingly, common for all autonomous

parvoviruses is that VP2 alone is able to assemble into empty (no DNA inside) capsid-like structures. For AAVs, empty VLPs generated from VP2 alone has been successfully expressed in insect cells (Ruffing et al. 1992). Empty VLPs of VP2 have also been generated successfully with CPV (Saliki et al. 1992), MEV (Christensen et al. 1993), human parvovirus B19 (Brown et al. 1991, Kajigaya et al. 1991) and MVM (Agbandje-McKenna et al. 1998, Hernando et al. 2000, Llamas-Saiz et al. 1997), which was discovered and isolated already in 1966 (Crawford 1966).

In B19, VP1 alone forms capsids with low efficiency, but in the presence of both structural proteins VP1 and VP2, the capsid structure is stabilized (Kawase et al. 1995). This supports the hypothesis that VP2 carries the majority of essential hydrogen bonds for correct capsid assembly. On its own, VP1 has shown to have other relevant functions, such as the motif for phospholipase A2 (PLA2) activity for many parvoviruses (Zadori et al. 2001). The catalytic PLA2 specificity in the B19 VP1 protein has originally been designated among three distinct amino acids 153 (His), 157 (Tyr) and 195 (Asp) (Arni & Ward 1996). The specific PLA2 activity also remained in the presence of empty recombinant VLPs containing both VP1 and VP2, but not in VLPs with only VP2 (Dorsch et al. 2002). VP1 has also been shown to possess other functions such as VP1 and its junctions between VP2 have shown to be a mediator for the action of neutralizing antibodies (Kawase et al. 1995). Additionally, B19 VP1 contains a unique region for binding to the erythrocyte cell surface receptor P antigen, when virus enters the host cell (Brown et al. 1993).

2.4.2 The structure of parvovirus

Some viruses have developed an effective way to construct capsids only of a few viral proteins, instead of forming capsids with a large number of different viral proteins (Damodaran et al. 2002). This is important when thinking of the coding efficiency that multiple proteins can be translated from the same, relatively short genomic sequence. In icosahedral symmetry, each subunit has to be located in structurally identical environments (Caspar & Klug 1962). All parvoviruses fulfill these criteria. Using overlapping reading frames, parvoviruses with a 5.6 kb genome have assured encoding a total of 3 viral structural proteins VP1, VP2 and VP3 required to form complete icosahedral capsids.

Parvoviral capsids have an outer protein layer consisting of 60 subunits. Each facet contains 3 viral protein subunits, arranged to a T=1 symmetry. Each viral protein has a “jelly-roll” antiparallel β-barrel structure (Tsao et al. 1991). It has also been assumed that the most conserved regions in the parvovirus genome would be located in these beta-barrels, and that the function of the recognition sites and the main sites for antigenicity would be located in more variable surface loops at the amino ends of VP1 and VP2 (Brown et al. 1992, Rosenfeld et al. 1992). The size for spherical parvoviruses varies with a diameter of 18-26 nm (Chapman & Rossmann 1993) depending on the species concerned. The structure of empty capsids of human parvovirus B19 derived from

baculovirus infected insect cells consisting only of VP2 has been resolved at 8 Å resolution, and the diameter determined to be 22-24 nm (Agbandje et al. 1994, Agbandje et al. 1991). The CPV capsid is composed of 60 subunits as a combination of both VP1 and VP2 (Weichert et al. 1998, Xie & Chapman 1996). The structure of CPV has also been resolved by X-ray crystallography with 3.25 Å and 2.9 Å resolutions, respectively (Tsao et al. 1991, Xie & Chapman 1996). The diameter of native CPV is approximately 26 nm (Agbandje et al. 1993, Yuan & Parrish 2001) and with only a 1 Å error in the icosahedral radius of the virion (Tsao et al. 1991). It is also notable, that full capsids of CPV are also very strong standing up to 65˚C of heat, and a wide range of pH (Suikkanen et al. 2003b, Vihinen-Ranta et al. 2002). Being relatively resistant to hostile environments, CPV capsids are excellent tools for studying viral entry and trafficking processes, since endosomes and lysosomes, the organelles on its route are all variable in pH. Naturally the N-terminus of VP1 is inside the virion of CPV. The activity of the parvoviral phospholipase A2 (PLA2) seems to increase when the pH is lowered (Suikkanen et al. 2003b). So, even though lowering the pH during cellular trafficking does not degrade the viral capsid, it does not mean that there are no structural changes. Exposure of the N-terminus of VP1 is a good example of that (Suikkanen et al. 2003b).

Protein-protein interactions are of important relevance in many fundamental events in biology. Much from these interactions inside multimeric, large complexes such as virus capsids remain still to be investigated (Reguera et al. 2004). The point mutations made to interfacial contacts between the intertrimeric subunits of VP2 in the MVM capsid have revealed that only a few relevant amino acids are responsible for assembly (Reguera et al. 2004) and that the majority of the atomic contacts between the amino acids in VP2 (104 aa from total 587 aa) are located inside the trimers (Agbandje-McKenna et al. 1998, Carreira et al. 2004, Chapman & Rossmann 1993, Reguera et al. 2004, Wu & Rossmann 1993). This suggests that the trimers form the intermediates in parvoviral subassembly and that the contacts inside these trimers are stronger than the bonds between the trimers. The small genome size has limited parvoviruses from carrying extra resources in order to express accessory proteins for viral entry and trafficking (Tsao et al. 1991, Xie & Chapman 1996) and thus the structure of the capsid itself has to provide these implications to carry out the functional signals for entry of the virus. Here, VP1 has a specific role common for many parvoviruses in the binding process of the capsid to the host cell surface. For CPV, VP1 has been shown to have a relevant role in nuclear targeting (Vihinen-Ranta et al. 2002).

2.4.3 Parvovirus life cycle

Viruses release their genetic contents inside the cells after the binding to the cell surface (Greber 2002). Among parvoviruses, CPV and B19 use different specific strategies with functional sites on their capsid surface, which involves receptor-mediated binding to the surface of host cells. Parvoviruses recognize different carbohydrates in the glycoproteins or proteoglycans at the cell surface. A region

formed by aa 577 to 677 in VP1 and VP2 of B19 binds to the cell surface receptor P-antigen (Brown et al. 1993, Dorsch et al. 2002).

Some parvoviruses use integrins co-operatively with viral receptors in binding. Integrins are a family of proteins belonging to widely expressed cell adhesion receptors that cells use to attach to extracellular matrices. B19 requires α5β1 integrin as a co-receptor for binding (Brown et al. 1993). It has been shown, that for both AAVs and CPV the internalization of the virus includes the formation of clathrin-coated pits by binding first to transferrin receptors (TfRs) (Parker et al. 2001). After attachment of the virus to the cell surface, many parvoviruses have been reported to use the endocytic machinery in trafficking towards the nucleus (Vihinen-Ranta et al. 2004). CPV enters through the cell membrane by clathrin-mediated endocytosis, which involves invagination of the cell membrane together with transferrin and forming large endosomes throughout the cell cytoplasm (Suikkanen et al. 2002). Both CPV, as well as FPV show the same pattern in binding and internalization (Parker et al. 2001). However, the endocytosis for CPV has not been shown to follow any routes concerning the endoplasmic reticulum or trans-Golgi network (Suikkanen et al. 2003b). The AAV serotype-2 uses heparin sulphate proteoglycan receptor molecules (HSPG) as recognition sites and AAV serotypes 4 and 5 sialic acids. Both of them require growth factor receptor (FGFR1) and integrin αvβ5 as co-receptors (Summerford et al. 1999).

Most of the DNA viruses replicate in the nucleus. In order for parvoviruses to be able to replicate, the host cell must be in S-phase (Brown et al. 1993). To release the viral genome from its protective shell, parvoviruses have to uncoat to enable the replication of the ssDNA in the nucleus for production of new progeny virus. Then, the mRNA coding for the viral proteins is transcribed from the viral DNA. Synthesis starts with viral early proteins, the non-structural NS1 protein possessing DNA binding and unwinding activities (Christensen & Tattersall 2002). Late proteins instead, are served for structure, e.g. capsid proteins, of the virion, which in case of parvoviruses are VP1, VP2, and in many cases VP3. Replication of viral DNA produces new parvoviral genomes to be incorporated to progeny virions (Hoque et al. 1999, Lombardo et al. 2000).

3 AIMS OF THE STUDY

Detailed characterization of viral and virus-like particle structures is of importance in the development of tools aimed at e.g. diagnostic, vaccine and gene delivery applications. By combining molecular cloning and single molecule detection techniques by FCS, it is possible to follow interactions, the size and the number of macromolecules from very low target concentration. This enables characterization of single proteins or macromolecular complexes.

The aims of this study were to characterize enveloped and non-enveloped viruses and virus-like particles displaying EGFP by FCS. In addition VLPs of B19 were incubated with human serum samples and the interactions were analyzed.

The specific aims of the study were:

1. To monitor the characteristics of structurally modified baculovirus particles and the number of fusion proteins on the viral surface

2. To develop a method characterizing antibody classes from acute and past-immunity serum samples with FCS

3. To monitor the diffusion properties of fluorescent VLPs of B19 human parvovirus-like particles and their interactions with human serum samples, and to gain more information about the number of fusions present in the fVLPs of CPV and B19

4. To evaluate the effects of amino terminal deletions on the assembly properties of VP2 of CPV

4 SUMMARY OF MATERIALS AND METHODS

Full details are found in the original publications (I-V).

4.1 Constructions of recombinant baculoviruses

4.1.1 Cloning of VP2 of CPV and B19, and fluorescent VLPs of B19

Amplified PCR products of the CPV VP2 gene (see Table 2 for primers) was cloned into the plasmid vector pSP73 (Promega, Madison, WI). The *Bam*HI/*Eco*RI digested fragment containing the VP2 coding sequence was further cloned into the corresponding sites of the vector pFastBacI (Gibco BRL, Grand Island, NY) (II). The B19 VP2 construct has been described previously (Kaikkonen et al. 1999) (II), as has, the construct for CPV EGFP-VP2 (III) (Gilbert et al. 2004). For generation of B19 EGFP-VP2 VLPs, the sequence encoding VP2 of B19 was produced by PCR and inserted into the *Hind*III/*Eco*RI sites of pEGFP-C1 (Clontech, Palo Alto, CA). In the resulting pEGFP-VP2-C1, EGFP-VP2 was placed under the polyhedrin promoter into pVP2FastBac resulting in plasmid pEGFP-VP2FastBac (IV).

4.1.2 Cloning of deletion constructs of fluorescent CPV VLPs

The truncated CPV VP2 gene constructs EGFP-VP2-14, EGFP-VP2-23 and EGFP-VP2-40 were cloned as follows. The sequence truncated by 14, 23 and 40 amino acids from the amino terminus of VP2 were amplified by PCR, isolated, and cloned into the plasmid pFastBacI (Gibco BRL). Further, this plasmid now containing now VP2 was used when EGFP was cloned. The amplification of EGFP has been described previously (Gilbert et al. 2004). PCR products of EGFP were then cloned into the previously constructed vectors with suitable restriction endonucleases resulting in plasmids pEGFP-VP2-14FastBac, pEGFP-

VP2-23FastBac and pEGFP-VP2-40FastBac (Fig. 6) (V). All used restriction enzymes were from MBI Fermentas (Vilnius, Lithuania).

TABLE 2 Sense and antisense primers used in the PCR reactions. Restriction sites are bold in Italic. *Bold characters in the gene construct describe the name of the sequence used for primers.

Gene construct*	Sense primer
EGFP-**VP2-40**	5'-GTG ***GGA TCC*** ATG TCT ACG GGT ACT TTC AAT AAT C-3'
EGFP-**VP2-23**	5'-GCT ***GGA TCC*** ATG GGG AAC GGG TC-3'
EGFP-**VP2-14**	5'-GGT ***GGA TCC*** ATG GTC AGA AAT GAA AGA GC-3'
EGFP-**VP2** (B19)	5'-G TCC GAA ***GCG CGC*** ATG GTG AGC AAG GGC-3'
EGFP	5'-GTC ***GGA TCC*** ATG GTG AGC AAG GGC G-3'
Gene construct*	Antisense primer
EGFP-**VP2** (B19)	5'-C GGC ACA ***CGT GGG*** TAA CCG CCG GCG GA-3'
EGFP-**VP2-14/23/40**	5'-CGA GGC GAA TTC TTA ATA TAA TTT TCT AGG TGC-3'
EGFP	5'-TAA ***AGA TCT*** CTT GTA CAG CTC GTC CA-3'

4.2 Cell lines, plasmids and generated viruses

For construction of plasmids to create recombinant baculoviruses prior to FCS analysis, competent *E.coli* JM 109 and DH10Bac cells were used (IV, V). Recombinant *Ac*GFPgp64 particles (I, III), empty human parvovirus B19 and CPV VLPs (II), or fluorescent VLPs of B19 and CPV VP2 (III-V) were all propagated in *Spodoptera frugiperda* 9 (*Sf*9) insect cells with the baculovirus system as follows. *Sf*9 cells were used to propagate recombinant baculoviruses in HyQ SFX culture medium (HyClone Inc, Logan, UT, USA). pFastBacI plasmid was used to amplify the genes of interest (VP2 or EGFP-VP2), resulting in plasmids pB19-VP2FastBac and pCPV-VP2FastBac (II), pEGFP-VP2FastBac (B19) (IV), deletion constructs pEGFP-VP2-14FastBac, pEGFP-VP2-23FastBac and pEGFP-VP2-40FastbBac (V). These vectors were used to produce recombinant baculoviruses with the Bac-to-Bac™ system (Gibco BRL). The Bac-to-Bac™ system uses site-specific transposition for insertion of foreign gene into baculovirus genome in *E.coli* DH10Bac cells, which allows the generation of recombinant baculoviruses (rBV). The resulting rBVs were designated as *Ac*B19-VP2 and *Ac*CPV-VP2 (II), *Ac*EGFP-VP2 (B19) (IV) and fluorescent VP2 – aminoterminal deletion mutants of CPV (*Ac*EGFP-VP2-14, *Ac*EGFP-VP2-23 and *Ac*EGFP-VP2-40) (V). Recombinant baculovirus *Ac*EGFPVP2 (CPV) containing a cassette coding for EGFP-VP2 (CPV), described previously (Gilbert et al. 2004) was used in the study (III). Budded virus, *Ac*GFPgp64 was produced directly from viral stocks (I, III). Viral stocks were produced either in monolayer or suspension cultures (125 rpm/min). Cells were infected at a multiplicity of infection (MOI) of 0.1 (I, III) or 3 to 10 (II, III, IV, V). Cells were harvested at three days post infection (p.i.) for the FCS analysis of budded virus *Ac*GFPgp64 (I, IV).

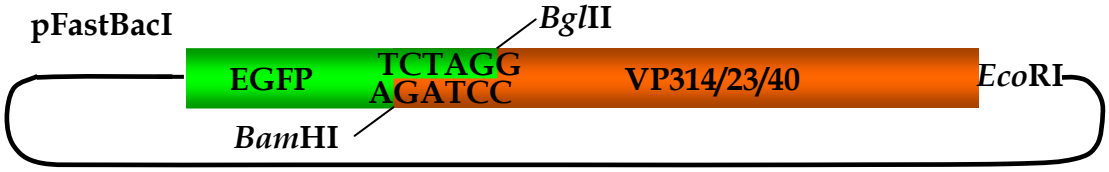

FIGURE 6 Schematic drawing of the plasmid construct used to generate rBVs.

4.3 Purification of recombinant viruses and VLPs

The *Ac*GFPgp64 virus was concentrated from the medium in three steps as follows: First, low-speed centrifugation of 600 x g for 5 min at 4 °C was performed. Second step was to clarify the supernatant by 6 000 x g for 15 min at 4 °C and thirdly, the BVs were concentrated at 100 000 x g for 30 min at 4 °C. The pellets of BVs were incubated in TE buffer (1 mM Tris, 0.1 mM EDTA, pH 7.4) overnight on ice and in order to avoid particle breakdown, they were resuspended gently prior to FCS analysis (I, III). The *Sf9* cells containing recombinant VLPs (II-V) were purified as follows: cells were concentrated at 1 000 x *g* for 10 min and solubilized in TENT buffer (50 mM Tris/HCl, 10 mM EDTA, 150 mM NaCl, 2 mM phenylmethylsulfonylfluoride, pH 7.4) at 4 °C into a density of 2.5 x 10^7 cells/ml after which cells were mixed with 0.2 % Triton X-100 followed by incubation on ice for 15 min. Cytoplasmic extracts were removed by a centrifugation step at 10 000 x *g* at 4 °C. VLPs were then concentrated by ultracentrifugation of the supernatant fractions at 100 000 x *g*. VP2 VLPs of B19 and CPV (II) were isolated by using $CsCl_2$ gradient ultracentrifugation. Sucrose gradient ultracentrifugation was performed to isolate fluorescent EGFP-VP2 B19 (IV) and constructs of EGFP-VP2, EGFP-VP2-14, EGFP-VP2-23 and EGFP-VP2-40 (V) VLPs as follows: the pellets were gently resuspended in 1 ml of ice-cold PBS containing 200 mM NaCl. 2 ml samples were carefully loaded on the top of 37 ml tubes containing 10 to 40 % weight/volume (w/v) of sucrose gradients and ultracentrifuged for 4 h at 102 000 x g, 4 °C. The fluorescent bands containing VLPs were detected visually under an UV light and extracted by a syringe. For further FCS characterization, the contents of the tubes were fractionated into 500 µl aliquots. Each aliquot was then dialyzed against PBS for 2 days at 4 °C and protected from light. For other use than FCS, samples were concentrated 200 000 x g, 1h at 4 °C and the resultant pellets were resuspended in buffer containing 50 mM Tris/HCl, 10 mM EDTA, 150 mM NaCl, 2 mM phenylmethylsulfonylfluoride, pH 7.4 (IV, V). Throughout the FCS analysis all viral samples were stored on ice and protected from light by covering them with foil (I-V).

4.4 Electron microscopy

Purified samples of B19 and CPV VP2 VLPs (II) and fluorescent VLPs (IV, V) were isolated from the sucrose gradient and used in electron microscopy studies. For negative staining, 20 µl samples were incubated on carbon-coated copper grids. Excess liquid was removed with Whatman 3MM filter paper prior to the addition of the negative stain (2 % potassium phosphotungstate, pH 6). After removal of excess stain, the grid was air-dried a few minutes, and monitored by transmission electron microscopy at 60 kV (JEOL JEM-1200 EX, Tokyo, Japan) (II, IV, V).

4.5 SDS-PAGE and Western blotting

The purified protein samples isolated from infected *Sf*9 insect cells (II, IV, V) were analyzed by SDS-PAGE using standard methods (Laemmli 1970) and blotted onto nitrocellulose sheets for immunodetection. To avoid unspecific binding, samples were blocked with 3% milk protein solution in PBS. Immunostaining with appropriate primary antibodies (Table 3) was followed by labeling the proteins with horseradish peroxidase (HRP) conjugated secondary antibodies (rabbit anti-human IgG), or alkaline phosphatase (AP) conjugated goat anti-mouse IgG (Promega) against mouse monoclonal antibodies (B19 VLPs) (II). CPV VP2 proteins were identified using polyclonal rabbit anti-CPV antibodies followed by labeling with AP-conjugated anti-rabbit IgG (II, V). The fusion protein (EGFP) presented in the EGFP-VP2 construct and in the corresponding amino terminal deletion constructs, were all detected with polyclonal rabbit anti-GFP antibodies (Promega). The sample proteins were detected from immunoblot sheets using color reaction with a substrate solution containing NBT and BCIP (Sigma-Aldrich). HRP was detected using 3,3'-diaminobenzidine tetrahydrochloride (DAB; ICN Biomedicals, Costa Mesa, CA, USA) and hydrogen peroxide as substrates. Molecular weight markers were from MBI Fermentas (II, IV, V).

TABLE 3 Primary antibodies used in this thesis.

Primary antibody	Target	Provider or reference	Source
Acute, past-immunity and negative serum	B19 virus	Dr. Klaus Hedman	human
anti-parvovirus B19	B19 virus	Dako, Glostrup, Denmark	rabbit
Anti-VP2, MAB8292	aa 446-466 of B19 VP2	Chemicon, Temecula, CA	mouse
anti-VP, Cornell#2	Structural proteins of CPV	Dr. Colin Parrish	rabbit
anti-capsid, A3B10	Intact CPV capsid	(Wikoff et al. 1994)	mouse
anti-capsid, A4E3	Intact CPV capsid	Dr. Colin Parrish	mouse
anti-GFP	EGFP	Promega, Madison, WI	rabbit

4.6 Enzyme Immuno Assay (EIA) measurements

Human serum antibodies against B19 VP2 were quantified using B19 virus-like particles in enzyme immuno assay (EIA) technique as previously described (Kaikkonen et al. 1999). The VP2-IgM antibodies against B19 were measured with a commercial EIA kit (Biotrin, Dublin, Ireland) (II).

4.7 Immunolabeling and confocal microscopy

The immunolabeling procedure was performed throughout at room temperature (RT). Infected *Sf*9 cells were pelleted briefly (800 x g, 1 min) and washed with PBS. Cells were further fixed with 50 µl of 4% PFA-PBS for 20 min. Concentrated cells were washed 3 times with 50 µl of 0.15 % glycine/PBS and centrifuged between each washing at 10 000 x g for 1 min. Cells from the feedings with fluorescent VLPs and from rBV infections (IV, V) were treated for 20 min with permeabilization solution (1% Triton X-100, 1% BSA and 0.01% sodium azide in PBS) and concentrated (10 000 x g, 1 min, RT). Cells were further incubated with corresponding primary antibodies A4E3 (mAb), anti-GFP (V), and anti-VP2 antibodies (IV), washed several times with PBS and detected by secondary antibody anti-mouse Alexa 633. Cells were embedded with 2-7 µl of MOWIOL-DABCO (30 mg/ml; Sigma-Aldrich). Cover slips were left for 2-24 h at 4 °C and studied using laser scanning fluorescence microscope with excitation wavelength for the dyes, and emission filters according to instructions of the manufacturer (Carl Zeiss Laser Scanning Microscope, Axiovert 100M, LSM 510, Jena, Germany). EGFP was visualized directly at excitation wavelength 488 (IV, V).

4.8 Fluorescence correlation spectroscopy

4.8.1 Setup

FCS was carried out in thermostated room at 22 °C using a fluorescence correlation microscope ConfoCorII (Carl Zeiss). The instrument was running in an autocorrelation mode, and for correct particle numbers and photophysical aspects, the counts per molecule (CPM), count rate (CR) and the triplet state populations of fluorescent dyes were adjusted and monitored according to the instructions provided by the manufacturer (Carl Zeiss). For the autocorrelation measurements of *Ac*GFPgp64 particles (I, III), fluorescent constructs of CPV [EGFP-VP2, EGFP-VP2-14, EGFP-VP2-23, EGFP-VP2-40 (V)] and B19 (EGFP-VP2 B19 VLPs) (III, IV), an Ar-ion laser at excitation wavelength of 488 nm was

used. Emitted photons were collected by using a 530-600 nm bandpass filter. The pinhole diameter was adjusted to 70 μm at 488 nm wavelength. For channel 2 at 543 nm excitation of the laser beam, an 80 μm pinhole radius was used. The correct structure parameter (SP) was obtained by optimizing the pinhole coordinates in the X, Y and Z direction with an automatic pinhole adjustment using Rhodamine 6G (Rh6G) (Molecular Probes, Eugene, OR, USA) at a count rate of 200 kHz with a laser power 0.1%. When the buffer solution η was changed during the measurements, the refractive index was fine-adjusted by using the correction ring of the instrument for optimizing maximal the CPM of the fluorescent particles. A HeNe-laser (543 nm) was used for the excitation of TMR and the emission was collected with a 560-615 nm bandpass filter (I). The laser beam was focused at 200 μm up from the glass bottom of the sample cuvette. All FCS experiments were carried out using 20 repeats and a measuring time of 20 seconds in LabTek® II 8-well chambered borosilicate glass plates (Nalge Nunc International, Naperville, IL, USA). The software of the instrument was used to calculate the autocorrelation function, diffusion time, and the number of particles per confocal volume element. Calibrated system with free dye molecules with corresponding pinhole settings and proper settings for emission and excitation filters were used. Calculations of the confocal volume element, diffusion coefficient and the hydrodynamic radii of particles were made as described in section 2.1.3.

4.8.2 Chemical and enzymatic treatment of viral nanoparticles

The fluorescent samples (I-V) were diluted in PBS or the buffer of choice to give at least 0.2 particles per confocal volume element and equilibrated for 5 min at 22 °C. All viral nanoparticles and tetramethyl Rhodamine (TMR) used in the experiments were analyzed by FCS before and after treatment with chemicals (I, III, V). Purified baculovirus particles, *Ac*GFPgp64, were exposed to different concentrations of n-Octyl β-d-Glucopyranoside (0.1-50 mM), Triton X-100 (0.01-3 mM), and SDS (0.01-5 mM) and further incubated at RT for 10 min. Particles were measured first 20 X 20 seconds each by FCS. The virus sample containing 5 mM SDS was further treated with 25 mM DTT (dithiotreitol) for 5 minutes and again analyzed with FCS (III). Soluble EGFP was used as a control for photophysical aspects, and again FCS -analyzed. 1 nM TMR dye (Fluoreporter® Tetramethylrhodamine Protein Labeling Kit, Molecular Probes) was exposed to 5 mM SDS prior to FCS analysis (I). Recombinant fluorescent VLPs of EGFP-VP2 (B19) (IV) or EGFP-VP2 (CPV) (III) and the deletion constructs EGFP-VP2-14, EGFP-VP2-23 and EGFP-VP2-40 were analyzed by 1-component model, and the diffusion constant was obtained averaging 6 times of repeated autocorrelations. According to the fitting algorithm processed by the ConfoCor2 software, the fractions with best fits were selected for further analysis. The particles were incubated for 15 minutes at 50 °C in the presence of 6 M urea and analyzed by FCS as follows: VLPs were mixed well in 200 μl volume, and divided into two tubes. One 100 μl aliquot was transferred to 6 M

urea and the other 100 µl to buffer only. When diluted for single-component analysis, VLPs in PBS were used. Dilution of 1:200 corresponded to 0.2 particles in the confocal volume element. After the 6M urea treatment, VLPs were diluted correspondingly to a final concentration of 0.03 M urea for FCS. 0.03 M urea did not affect the measured diffusion time and thus 0.03 M urea did not change the viscosity. Deletion constructs were also treated (5 min) in the presence of 8.3×10^{-13} M of trypsin at RT and then analyzed by FCS (V). For EGFP-VP2 (B19), VLPs were treated with 5 mM SDS followed by FCS analysis (III, IV). All samples were stored on ice before measurements, and equilibrated for 10 min at 22 °C prior to FCS.

4.8.3 Binding of B19 VLPs to the serum antibodies

The binding of acute-phase, past-immunity serum and negative serum samples to the VP2 VLPs of B19 was evaluated as follows: after labeling the VLPs with Oregon Green 488, VLPs were purified through a Sephadex™-G50 gel filtration column. After collecting peak fractions with UV-monitor from the gel filtration, they were analyzed by FCS. Translational diffusion time of the free dye molecules was first measured with a one-component model. This value was then fixed, and the diffusion time of Oregon Green 488 -labeled VP2 particles was obtained with a two-component model using the software of ConfoCor2 instrument. Autocorrelation analysis was performed by using the fitting software of the FCS device. The fractions with no aggregates with best fits corresponding to the size of VLPs were selected for further studies. The interaction of the human serum samples with the VLPs was measured with 40 repeats of 20 s each. The binding experiments were carried out at low serum concentrations (1: 30 000) in order to avoid background noise (data not shown) of autofluorescent protein components arising from the original, concentrated serum. The result was fitted with the two-component model provided by the manufacturer's software and the binding of the antibodies to the VP2 VLPs was evaluated.

The fluorescence autocorrelation functions for all measured experiments (I-V) were performed with 40 or 20 repeats using a 20 s measuring time. For the averaged autocorrelation experiments, and the mean deviations for all the measured diffusion times, FCS experiments were repeated identically at least 6 times. From the changes in the amplitude of the autocorrelation curve the particle number in the confocal volume element was calculated. Normalized correlation curves were used except in paper I. Hydrodynamic radii of all samples (I-V) were calculated by Stokes-Einstein –equation described in section 2.1.3 of this thesis. All detergents were from Sigma-Aldrich (I-V).

4.8.4 Labeling procedures

400 µg (0.4 mg/ml) of B19 VLPs (II) were labeled with Oregon Green 488 succinimidylester using 2-4 moles of dye per one mole of protein according to the instructions of the manufacturer (Molecular Probes). The labeled B19 VP2

VLPs were separated from the impurities using gel chromatography (Sephadex™ G-50, Amersham Biosciences AB, Uppsala, Sweden) and equilibrated against 0.1 M $NaHCO_3$ (pH 8.3). The fractions were collected using UV (A_{280}) -detection (Single Path Monitor UV-1, Amersham Biosciences) and fluorescence spectroscope (Wallac VICTOR² D Fluorometer, Perkin Elmer Life Sciences Inc., MA, USA). Protein concentration of the VLPs was carried out by standard procedures (Bio-Rad protein assay). The fractions were further characterized by SDS-PAGE and immunoblot analysis as previously described. The labeled and purified VLPs were used directly in FCS measurements. After dialysis, the sample was diluted 1:100 in PBS and the FCS analysis of single CPV particles was carried out as described.

5 REVIEW OF THE RESULTS

5.1 Presence of GFPgp64 on the envelope of *Ac*GFPgp64

5.1.1 Diffusion of the *Ac*GFPgp64 in solution

Analysis of the fluorescent baculovirus *Ac*GFPgp64 for FCS started with the production and purification of the respective budded virus displaying GFP fused to the membrane anchor protein gp64. Immunoblotting of the fusion protein of this virus has previously been described in detail (Mottershead et al. 1997). The goal of this work was to determine diffusion properties of an enveloped virus *Ac*GFPgp64 by FCS including the presence, the number and the size of chimeric fusions on the surface of the virus (I, III). For the intact *Ac*GFPgp64 -particle at 22 °C, calculations of the measured diffusion time of 3.3 ms through a 0.2 fl confocal volume element corresponded approximately to a hydrodynamic radius of 83 nm, however with a high deviation (± 21 nm) (Table 4). It is reasonable that a rod-shaped particle like baculovirus would be expected to have a diffusion pattern with a high deviation since the virus can vary significantly regarding the number of protein molecules packed helically in the inner nucleocapsid (Burgess 1977). This will certainly contribute to the mean size of a large number of viruses detected in the solution, since the shape of the envelope follows the changes in the size of the nucleocapsid. This was also indicated by the corresponding diffusion time for the intact virus, which deviated by 25% (Table 4). Despite this, the measured size for the virion corresponded generally very well with the previously determined size of wild-type baculovirus 50 nm x 250 nm (Fraser 1986). However, there was a reproducible decay in the curve at 100 ms range (I, Fig. 1), which resulted in a poor fit at that range (data not shown). The autocorrelation decay in that range possibly represents viral aggregated material or laterally moving fluorescent molecules on the viral surface, and could not thereby be resolved by fitting into the two-component model (I, III).

5.1.2 Presence of fusion protein on the baculoviral membrane

In order to evaluate the number of GFP-labeled protein composition buried in the lipid bilayer, the virus was degraded by using detergents at the concentration range close to critical micellar concentration (CMC) (SDS 3 mM). Although the diffusion constants for any baculoviruses and its proteins have not been previously reported, it would not be unreasonable for a gp64 trimer-detergent complex to move with a protein mass of 180 kDa (Trier et al. 1999) through the confocal volume element with a hydrodynamic radius of approximately 5 nm (Table 4). To distinguish two different sized fluorescent populations simultaneously by FCS, at least 1.6 to 2– fold differences in the diffusion times has to be obtained. This criterion was fulfilled, when the measured diffusion time of the fusion protein was 15-fold smaller (0.2 ms) compared to the intact *Ac*GFPgp64 virion (3.3 ms). By using detergents, the average number of fluorescent species per one virion could be measured from the changes in the amplitude. There was a decrease in the amplitude corresponding to a 3-fold increase in the particle number, and a notable change in diffusion time and hydrodynamic radius from 83 nm to 5 nm. In the case of SDS and Triton X-100, a dissolving effect was observed at detergent concentrations lower than CMC (Table 4) (I, III).

TABLE 4 Particle, diffusion times before (τD1) and after (τD2) treatment with chemicals at RT, hydrodynamic radii before [Rh (D1)] and after [Rh (D2)] treatment with chemicals at RT and the number of fluorescent particles per baculovirus *Ac*GFPgp64 (*N*f) studied in this thesis.

Particle	τ_{D1} (ms)	τ_{D2} (ms)	$R_{h(D1)}$ (nm)	$R_{h(D2)}$ (nm)	N_f
*Ac*GFPgp64 (3 mM SDS)	3.3 ± 0.8	0.2 ± 0.0	83.0 ± 19.0	4.6 ± 0.5	3.0 ± 0.0
*Ac*GFPgp64 (25 mM DTT)	0.2 ± 0.0	0.1 ± 0.0	4 .6 ± 0.5	2.5 ± 0.4	4.5 ± 0.0
sEGFP	0.1 ± 0.0	0.1 ± 0.0	2.0 ± 0.1	2.0 ± 0.1	1.0 ± 0.0

5.1.3 Disulphide bonds present in the gp64-fusions

The analysis of viral breakdown products was continued after SDS treatment further with a reducing agent, DTT, at RT (III, Table 1). Generally, DTT has an effect on breaking down the disulphide bonds (-S-S-) between cysteines that keep globular proteins folded. The presence and the location of intramolecular disulphide bonds are key determinants in the function and structure of proteins (Hartig et al. 2005). The effect of 25 mM DTT in the presence of 3 mM SDS increased the total number of fluorescent particles by a factor of 1.5 in the enveloped virus *Ac*GFPgp64 (Table 4). This probably means that on the average there are 1.5 smaller units connected by disulphide bonds. These units could be gp64 glycoproteins. It is known that anchor protein gp64 is present as disulphide-linked trimers at the membrane (Markovic et al. 1998). Although the number of gp64 protein molecules present in the wild-type baculoviral envelope is not known, it is known that only a minor proportion of the fusion product is substituted at the membrane (Grabherr et al. 1997, Grabherr et al.

2001, Mottershead et al. 1997, Ojala et al. 2001). However, the number of unlabeled gp64 molecules in this study was not determined, meaning that there is a possibility of those unlabeled proteins making also dimers or trimers together with the fusion proteins at the viral membrane. Moreover, reduction with DTT revealed products smaller (2 nm) than was expected with SDS alone (4 nm), which gave a result of the fusion protein being bigger than GFP alone (Table 4) and that they were distinguishable from each other (III).

5.1.4 Effect of detergents on the properties of soluble GFP

As a control for the contribution of detergents to the photophysical aspects, soluble GFP was measured in the presence and absence of 3 mM SDS. When GFP was measured, only minor changes in the diffusion time, counts per molecule (CPM) or in the amplitude of the autocorrelation function were detected. Diffusion time of GFP remained close to 0.1 ms in all studied concentration ranges, from 0.01 to 5 mM SDS. In the SDS concentration below 3 mM CPM was approximately 7 kHz, but was decreased to 6 kHz after 3 mM. Likewise, the amplitude G (t) was 3 in all concentrations from 0.01 to 5 mM of SDS and thus did not change (I, Fig. 5A and B) (I, III).

5.2 Characterization of the CPV and B19 viral proteins by standard techniques

To demonstrate the presence of VP2 in recombinant B19 VLPs, samples were stained by Coomassie brilliant blue followed by western blotting. Purified proteins of the expected size (58 kDa) were observed (II, Fig. 1). The constructs EGFP-VP2 (B19) (III, IV), EGFP-VP2 (CPV) with the corresponding VP2-aminoterminal deletions (EGFP-VP2-14, EGFP-VP2-23 and EGFP-VP2-40) (III, V) were all propagated in baculovirus infected insect cells and purified by using density ultracentrifugation sucrose gradient. The visually seen VLPs collected from the ultracentrifugation tube were clearly distinguished as bands from those free proteins at the top of the gradient (data not shown). For the validation and the expression of the CPV VP2 and EGFP in the constructs EGFP-VP2, EGFP-VP2-14, EGFP-VP2-23 and EGFP-VP2-40 and EGFP, were also characterized by western blotting. In all constructs, the presence of both VP2, and the EGFP in the fusion, was detected (V, Fig. 2A and B). EGFP-VP2 VLPs were detected with the polyclonal rabbit anti-VP2 antibodies against VP2 and, polyclonal rabbit anti-GFP antibodies against EGFP (Promega). All EGFP-VP2 fusions and VP2 and were moving with an apparent molecular weight of 94 and 64 kDa, correspondingly (V, Fig. 2A and B). No detectable differences in molecular weights between the VP2 and the deletions VP2-14, VP2-23 and VP2-40 were seen, since the lower bands below the distinctive VP2 bands were at the same distances from each other (V, Fig. 2A). The Recombinant B19 proteins VP1

and VP2, as well as soluble EGFP in the case of the fluorescent construct EGFP-VP2 of B19 migrated with the expected molecular weights, i.e., 83, 58, and 26 kDa, respectively. In addition, the EGFP-VP2 fusion protein migrated with an apparent molecular weight of 84 kDa as predicted (IV, Fig. 2). The observation of correct capsid formation of B19 VP2 VLPs was confirmed by electron microscopy (EM) (II, Fig. 2A and B). Particle diameters for B19 VLPs were approximately 19 nm (Table 8) (unpublished data, Patrik Michel, master's thesis work). The size and the shape of the corresponding VLPs resembled those previously measured (Kajigaya et al. 1991, Tsao et al. 1991, Yuan & Parrish 2001). The size of the constructs EGFP-VP2, EGFP-VP2-14, EGFP-VP2-23 and EGFP-VP2-40 were all confirmed by EM (V, Fig. 4B). The size of these VLPs resembled closely the size of wild type viruses measured by other investigators (Tsao et al. 1991, Wu & Rossmann 1993).

5.3 Monitoring VLP-antibody interactions by FCS

5.3.1 Binding of the human antibodies to the B19 VLPs

In the second article of this thesis, binding of human parvovirus B19 VLPs and antibodies present in acute-phase, past-immunity, and seronegative serum samples at very low concentration was studied using FCS (II). The binding was monitored using normalized autocorrelation curves by an autocorrelation analysis, as the binding of the antibodies with VLPs seemed to shift the curve to the right. Alexa 488 labeled and purified VLPs were measured by FCS. The measurement gave a hydrodynamic radius of 14 nm. The autocorrelation was measured from the reaction mixture with the corresponding serum at 13 min intervals after adding the corresponding serum. Both acute and past-immunity serum samples from 3 different persons were measured by FCS with the same results, but only one binding curve from one sample is shown. There was a clear shift of the autocorrelation curve to the right (Fig. 8A and 8B). The binding was observed in both cases 13 minutes after adding positive serum of choice. Oregon Green 488 labeled VLPs moved with a diffusion coefficient of 1.7×10^{-11} m^2s^{-1} and with a corresponding radius of 14 nm. The hydrodynamic radius corresponds very well to the data previously measured by other methods such as EM (Brown et al. 1991). In the presence of past-immunity serum the diffusion time of the first component was fixed and two-component analysis was performed. A mean τ_{diff}-value of 2.7 ms was measured. This corresponds to a diffusion coefficient of 3.5×10^{-12} m^2s^{-1} and a hydrodynamic radius of approximately 70 nm (Table 5). For the acute-phase serum, a mean τ_{diff}-value of 6.2 ms was obtained corresponding to D of 1.5×10^{-12} m^2s^{-1} and a hydrodynamic radius of approximately 160 nm. No binding was observed in the presence of control sample devoid of B19 VP2 specific antibodies, as can clearly be seen from the normalized autocorrelation (II, Fig. 4A). From the measured amplitude, the number of virus-like particles could also be calculated. The

observed number of 0.6 particles per confocal volume element corresponds approximately to 4 nM solution of VLPs, and after binding, 0.1 particles - 500 pM solution for a detected complex (II).

TABLE 5 Particle/serum, diffusion times before (τD1) and after (τD2) adding corresponding serum, diffusion coefficients for the complex (*D*), hydrodynamic radii in the absence [Rh (D1)] and in the presence [Rh (D2)] of past-immunity serum (VLP-ab past-imm), acute phase serum (VLP-ab acute), or negative serum (VLP-ab neg) and the number of fluorescent particles in the confocal volume element (*n*).

Particle/serum	τ_{D1} (ms)	τ_{D2} (ms)	D (m^2s^{-1})	$R_{h(D1)}$ (nm)	$R_{h(D2)}$ (nm)	n
VLP-OG 488	0.5 ± 0.1	-	1.7×10^{-11}	14 ± 3	-	0.6
VLP-ab neg.	0.5 ± 0.1	0.6 ± 0.1	1.6×10^{-11}	15 ± 2	15 ± 2	0.5
VLP-ab past-imm.	0.5 ± 0.1	2.7 ± 1.1	3.5×10^{-12}	14 ± 3	69 ± 27	0.2
VLP-ab acute	0.5 ± 0.1	6.2 ± 6.0	1.5×10^{-12}	14 ± 3	157 ± 151	0.1

5.4 Characterization of fluorescent B19 and CPV VLPs

5.4.1 Size of the fluorescent VLPs

In order to evaluate the number of the fusion proteins present in the VLPs, the diffusion properties of viral recombinant nanoparticles of EGFP-VP2 of B19 (IV) and the constructs EGFP-VP2 and the aminoterminal deletions EGFP-VP2-14, EGFP-VP2-23 and EGFP-VP2-40 of CPV were all studied by FCS (V). EGFP-VP2 (B19) VLPs diffused with Brownian motion in solution in 0.6 ms time through the confocal volume element, while EGFP-VP2 (CPV) diffused in 0.7 ms. For both the EGFP-VP2 (B19) and EGFP-VP2 (CPV) VLPs, the diffusion times corresponded to the *D* –values of 1.8 and 1.4 x 10^{-11} m^2s^{-1} and hydrodynamic radii of 14 and 17 nm, respectively. Standard deviation was 4 nm higher for EGFP-VP2 (CPV) (Table 6) which may suggest some stability problems in assembled capsids.

TABLE 6 Particles, diffusion times (τD1), diffusion coefficients before a treatment with 3 mM SDS at RT or 6 M urea at 50 °C (*D*1), hydrodynamic radii before [Rh(D1)] and after [Rh(D2)] a treatment with 3 mM SDS at RT or 6 M urea at 50 °C, and the number of fluorescent units per VLP (N_f).

Particle	τ_{D1} (ms)	D_1 (m^2s^{-1})	$R_{h(D1)}$ (nm)	$R_{h(D2)}$ (nm)	N_f
EGFP-VP2 (B19)	0.6 ± 0.1	1.8×10^{-11}	14 ± 2.4	4.8 ± 0.1	9.0 ± 5.0
EGFP-VP2 (CPV)	0.7 ± 0.3	1.4×10^{-11}	17.0 ± 7.0	8.5 ± 2.7	9.5 ± 0.7

Several deletions were introduced into the aminoterminal site of VP2 of CPV followed by a fusion with EGFP C-terminus. The resultant constructs EGFP-VP2, EGFP-VP2-14, EGFP-VP2-23 and EGFP-VP2-40 were purified in sucrose gradients and analyzed by FCS. The effect of deletions to capsid assembly properties was further characterized by using FCS (V, Fig. 6A-E). Fluorescent

constructs EGFP-VP2, EGFP-VP2-14, EGFP-VP2-23, EGFP-VP2-40 and soluble EGFP were all diluted in PBS in particle number of 0.2 per confocal volume element and analyzed by the one-component model of the autocorrelation of FCS. The diffusion time was close to 1 ms for EGFP-VP2, EGFP-VP2-23 and EGFP-VP2-40 –constructs (V, Figs. 6A, 6C-D). Values for the diffusion coefficient *D* were calculated according to the Stokes-Einstein equation (Eq. 3). Diffusion coefficients for all fVLPs of CPV and B19 were all in a range from 1.4 x 10^{-11} m^2s^{-1} to 1.2 x 10^{-11} m^2s^{-1}, corresponding to hydrodynamic radii of 14-20 nm (Table 6 and 7) (III-V).

5.4.2 Number of fusion proteins present in the fluorescent VLPs

The number of fluorescent units per one capsid for different fluorescent constructs was measured. When EGFP-VP2 (B19) was analyzed in the presence of 3mM SDS, the number of fluorescent particles was increased by a factor of 9 (IV). The control for photodynamic contribution of SDS to the brightness of EGFP particles was validated in article I. After incubation of CPV constructs EGFP-VP2, EGFP-VP2-23 and EGFP-VP2-40 in 6 M urea for 15 minutes at 50 °C, the hydrodynamic radius was reduced to 14 nm with a simultaneous 6 to 10 - fold increase in the particle number (Table 7). For the construct EGFP-VP2-14, the diffusion time was around 0.3 ms (V, Fig. 6B). When the deletion construct EGFP-VP2-14 was analyzed, the calculated diffusion coefficient of 3.6 x 10^{-11} m^2s^{-1} extracted from the fluorescence intensity autocorrelation function was much smaller than that of the capsid forming constructs, EGFP-VP2 (CPV), EGFP-VP2-23 and EGFP-VP2-40 (Table 7). The hydrodynamic radius for EGFP-VP2-14 was 7 nm. Followed by exposure of EGFP-VP2-14 at 50 °C and 6 M urea, the particle number was increased by a factor of 2. As well, these particles showed a diffusion coefficient of 6.2 x 10^{-11} m^2s^{-1}, which matches quite well with a diffusion coefficient expected for a globular protein with a size of about 85 kDa (Table 7 and V, Fig. 2A). EGFP-VP2-23 and EGFP-VP2-40 showed somewhat larger capsid structures than expected (Table 7) (V).

TABLE 7 Particles, diffusion times (τD1), diffusion coefficients before a treatment with 6 M urea at 50 °C (*D*1), hydrodynamic radii before [Rh(D1)] and after [Rh(D2)] a treatment with 6 M urea at 50 °C, and the number of fluorescent units per VLP (N_f).

Particle	τ_{D1} (ms)	*D*1 (m^2s^{-1})	$R_{h(D1)}$ (nm)	$R_{h(D2)}$ (nm)	N_f
EGFP-VP2 (CPV)	0.7 ± 0.3	1.4 x 10^{-11}	17.0 ± 7.0	8.5 ± 2.7	9.5 ± 0.7
EGFP-VP2-14	0.3 ± 0.0	3.6 x 10^{-11}	6.7 ± 0.9	3.9 ± 2.3	2.0 ± 0.1
EGFP-VP2-23	0.8 ± 0.2	1.2 x 10^{-11}	20.0 ± 4.0	10.0 ± 2.5	5.8 ± 1.3
EGFP-VP2-40	0.5 ± 0.1	1.8 x 10^{-11}	14 ± 3.4	9.0 ± 0.7	9.7 ± 0.1

8.3 x 10^{-13} M trypsin treatment for truncated CPV particles showed no difference in the particle number compared to those observed with 6 M urea and treatment at 50 °C (data not shown). Interestingly, the diffusion time was decreased ten-fold, from 0.8 ms to 0.08 ms (V, Fig. 8 A-C).

6 DISCUSSION

6.1 Size of *Ac*GFPgp64 displaying GFP analyzed by FCS

In previous reports FCS has been used in characterizing EGFP and GFP diffusing in intracellular environments (Brock & Jovin 1998) as well as in the nucleus (Wachsmuth et al. 2000). Molecular characterization has been especially addressed to monitoring photophysical dynamics of GFP (Widengren et al. 1999). For the purpose of biological interactions, FCS has also been utilized in studying molecular affinities and binding rate constants at cell surfaces (Pramanik et al. 2001), which makes this approach attractive when thinking of viral attachments at the cell surface. FCS has also been successfully used in measuring various diffusion constants *D*, which closely relates to the actual size of the particle (Yoshida et al. 2001). In the present study, fluorescent baculovirus *Ac*GFPgp64 –particles displaying GFP were monitored *in vitro* by FCS. Gp64 plays an important role in the baculovirus life-cycle. Successful targeting of the virus to the cell surface prior to entry is mediated by this molecule. A fusion protein, GFPgp64, has successfully been expressed under the control of polyhedrin promoter in insect cells (Mottershead et al. 1997, Ojala et al. 2001) and has been utilized further in binding studies with mammalian cells (Ojala et al. 2001). Article I in this thesis characterizes diffusion properties and the size of the recombinant GFP-displaying virus *Ac*GFPgp64 and the number of chimeric proteins on the membrane of the virus, as well as the diffusion of EGFP itself. The diffusion coefficient for EGFP (III, Table 1) was in very good agreement with previously reported investigations (Widengren et al. 1999). The apparent hydrodynamic radius of the baculovirus particle, as well as the amount of virus particles in the confocal volume element and the number of gp64 fusion proteins incorporated into the viral membrane could be determined. However, the number of those non-chimeric viruses was not determined. *Ac*GFPgp64 diffused in solution with a hydrodynamic radius of 83 nm albeit with a large standard deviation (Table 4). Finally, the presence of disulphide bonds revealed that there is more than one fluorescent species

present in the viral chimeric anchor protein GFPgp64 (IV). The characterization of the dynamic properties of this virus may allow the use of this approach, when the diffusion of the virus inside cells is concerned.

6.2 Number of fusion proteins on the baculoviral membrane

In addition to characterizing the size of macromolecules, the method has previously also been used to monitor changes in the number of fluorescent particles (Chen et al. 1999, Schwille et al. 1997a) in the confocal volume element of FCS. In the present study, after using the reducing agent dithiotreitol (DTT), 4.5 fluorescent units per one virus particle in the confocal volume element were detected. It is noteworthy that in FCS the averaged information is collected from a large number of single molecule fluctuations, whereas traditional research methods, such as fluorescence microscopy and confocal microscopy, characterize an ensemble of viruses or macromolecules simultaneously. Of traditional methods electron microscopy can also be used as a single particle approach, when particle size is concerned. To monitor single particle fluctuation, it was an advantage to monitor the presence of low number of fusion proteins incorporated in the viral membrane of *Ac*GFPgp64. The membrane protein gp64 has an important role, when the virus infects the host cell. In the future, information on the presence and the number of proteins on the viral membrane could be helpful, e.g. when monitoring baculoviral infection processes.

For baculoviruses, that needs to be studied urgently to develop new methods for gene delivery or targeting e.g. in cancer treatment, specific surface display peptides are being developed. These FCS studies presented in this thesis provide an alternative way for monitoring enveloped viruses and the number of fusion proteins on the surface of enveloped baculovirus. Thus, this approach could be useful, when the amount of proteins on the surface of enveloped virus are relevant e.g. for tumor targeting (I, III). To our knowledge, this study is the first where FCS has been utilized for studying a membrane glycoprotein anchored on the envelope of a viral particle (Fig. 7).

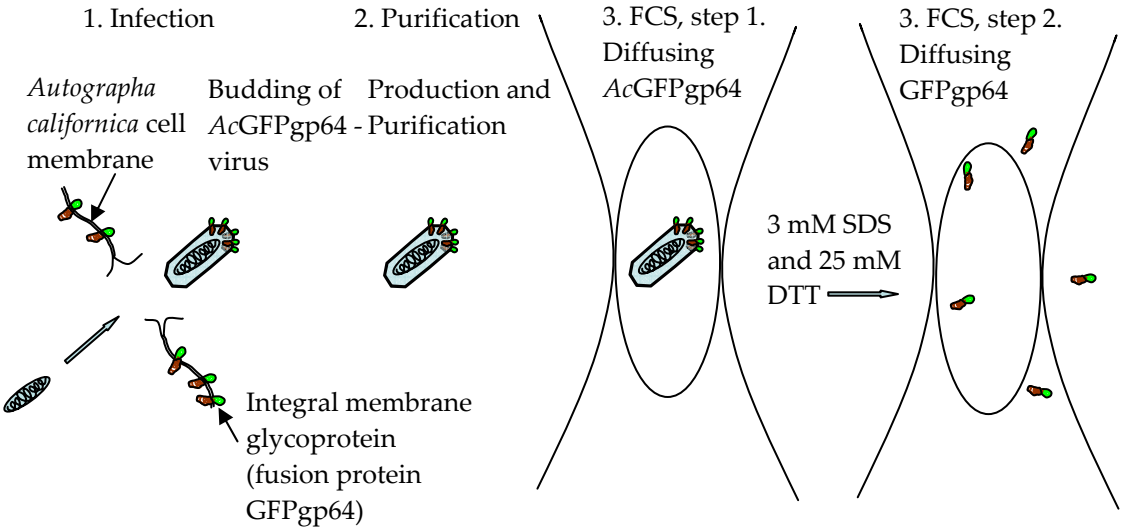

FIGURE 7 Measurement of diffusion time of *Ac*GFPgp64 by FCS.

6.3 Complexes of B19 serum antibodies and B19 VLPs

Human parvovirus B19 is harmful to humans. However, since recombinant VLPs (assembled from B19 structural proteins VP2 or VP1/VP2) are non-infectious, they have shown to be a promising tool for a variety of applications such as in the development of vaccines (Franssila & Hedman 2004). B19 VLPs have also been successfully utilized in studying the roles of B19 in targeting to specific cellular compartments by using VLPs of VP2 fused to EGFP (IV). In this thesis, the VLPs of human parvovirus B19 were used in the detection of antibody-VLP associations. Recombinant VLPs of VP2 produced in insect cells were semi-purified, labeled with Oregon Green 488, and characterized in the presence or in the absence of acute-phase and past-immunity serum samples by using FCS. The size of the purified particles were close to those measured by EM (unpublished data, Table 8) (Michel 2002);

TABLE 8 The diameter of B19 VLPs detected by EM. Unpublished data adapted from (Michel 2002)

Data	EM diameter (nm) B19				
	Mean	Median	Std deviation	Min	Max
	18.75	18.94	1.80	14.13	21.93

The number of VLPs observed in the confocal volume element was 0.6 (Table 5.) corresponding approximately to a 4 nM solution of VLPs. By using a solution of B19 VLPs close to nanomolar concentration and adding either acute or past-immunity sera, VLP-antibody reactions could be detected. The size of the complex for both acute, as well as for past-immunity serum after 13 min of incubation was much larger than that of the VLPs alone (Table 5). For an

accurate and reliable measurement, at least 0.1 particles per confocal volume element have to be obtained (Schwille et al. 1997a), since lowering the number of the particles from this will substantially decrease the SNR. Too rare emission bursts are harder to correlate and Raman scattering from the water molecules will become dominating in the autocorrelation. For acute-phase sera, it was evident, that a 5-fold decrease in the particle number in the observation volume resulted from specific binding of the antibodies present in the sample (Table 5). Also, in the presence of past-immunity sera, a 3-fold decrease in the particle number was observed compared to the Oregon Green 488 -labeled VLPs alone (Table 5). Non-specific binding was validated in the presence of seronegative serum sample, where no binding were observed. The results presented suggests that FCS is a sensitive method for analyzing virus-antibody interactions and that the antibodies present in the acute phase or past-immunity serum samples of B19 can directly be used in this assay. The shape of autocorrelations presented in Figure 8 makes it obvious, that the aggregations contribute largely on the curve, worsening the fit (data not shown). This is also evident from the high deviation in the complex size (Table 5) and the shape of the correlation curve at ms–range longer than 10 ms. When the two autocorrelation curves of VLPs for both the acute-phase sera components as well as the past-immunity sera are compared, major differences in the size of aggregations were detected. Acute-phase serum antibodies did form larger complexes than the antibodies present in the past-immunity serum. This was clear from both the measured diffusion times and corresponding decreased particle numbers (Fig. 8, Table 5). Additionally, after 26 min of incubation the amount of fluorescent VLPs had decreased 5-fold (Fig. 8, Table 5). Maximum complex size with acute-phase serum was achieved in 39 min, as can essentially be seen from the shape of the normalized autocorrelation curve in Figure 8A.

Antibodies present in acute phase sera after infection consists mainly of the antibody class IgM. Past-immunity serum is mainly occupied by IgG, however with a small amount of IgM. The immunoglobulin classes differ in their binding capacity, IgM consisting of 10 binding sites and IgG only of 2. Higher binding capacity may be a reason for larger deviation of the measured complex size for acute-phase serum (Table 5). These results clearly demonstrate that the antibodies present in the acute or past-immunity phase sera are capable of rapidly forming aggregates in the presence of B19 VLPs, and that the binding is observed by FCS already at 13 min after adding antibody mixture containing the target antibodies towards B19 VLPs. The acute-phase serum used was shown to contain IgM using EIA–measurement (II, Table II). Thus, FCS could be used to distinguish the immunoglobulin classes IgM and IgG (in serum samples) by detecting diffusion times of VLP-antibody complexes. The method may in future have applications also in fast virus detection (II).

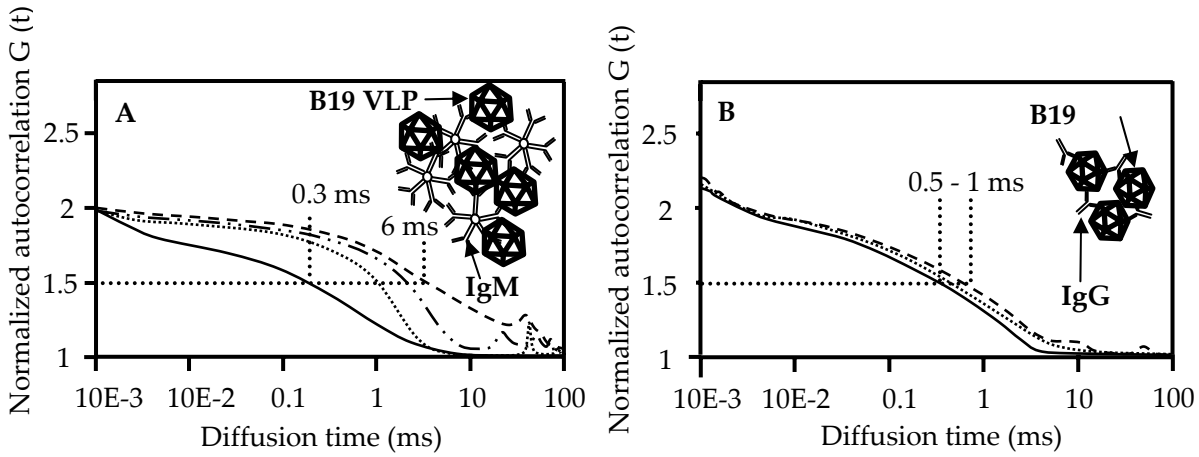

FIGURE 8 Schematic drawing of diffusion of labeled B19 VLPs in the presence of acute-phase (0.3 ms; VLP, 6 ms; formed complex at 39 min) (A) and past-immunity (0.5 ms; VLP, 1 ms; formed complex at 39 min) (B) serum components. Inset: formed antibody–VLP complexes. Figure is adapted and modified from the original article II.

6.4 Disassembly of fusions from fluorescent VLPs of CPV and B19 parvovirus

EGFP-tagged viral particles are under study, when tools for safe gene therapy are being developed. Recently, Lux and co-workers demonstrated that AAVs equipped with GFP-VP2 fusion protein were capable to produce high titer viruses (Lux et al. 2005). This proofs, that EGFP can be used as a natural marker to follow viral trafficking. By fusing GFP to the structural protein, fluorescent rotaviruses have been created without affecting capsid assembly (Charpilienne et al. 2001). In the present studies, diffusion properties of the fluorescent VLPs of both CPV and B19 were characterized by using FCS (IV,V). The size of the non-enveloped chimeric viruses displaying EGFP was studied, as well as with respect to the number of the fusion proteins disassembled from the VLPs (V, VI) after denaturation. Fluorescent non-enveloped VP2 VLPs of B19 (IV, III) and CPV (III), as well as the VP2 aminoterminal truncated versions (V) (EGFP-VP2-14, EGFP-VP2-23 and EGFP-VP2-40) were used in the FCS study to characterize the number of fluorescent fusions present in the capsid. Additionally, comparisons were made to the size of the VLPs, when studying the effects of deletions on the assembly properties of VP2 CPV (V, Table 1). Therefore, the amino terminus of the VP2 protein was truncated by 14, 23 and 40 amino acids. Corresponding aminoterminal truncations were further fused to the carboxyl-terminus of EGFP; the resulting protein products were expressed in insect cells and purified. In order to analyze the corresponding deletion mutants EGFP-VP2, EGFP-VP2-14, EGFP-VP2-23 and EGFP-VP2-40, Western blots for all constructs were performed and the corresponding molecular weights for EGFP and VP2 were obtained (V, Fig. 2). Purified VLPs were characterized by FCS.

The full length construct EGFP-VP2, and the constructs deleted from VP2 aminoterminus by 23 or 40 amino acids were able to assemble correctly (Table 6 and 7). Particles moving were detected by FCS with diffusion constants roughly corresponding to VLPs, but in the case of EGFP-VP2-14, where 14 amino acids deleted, no assembly was seen. EGFP-VP2-14 showed a particle radius of approximately 7 nm, which could be the size of the soluble fusion protein. This suggests that EGFP-VP2-14 lacks the capability to form capsids. The fusion proteins EGFP-VP2, EGFP-VP2-23 and EGFP-VP2-40 however did form capsids (V, Figs. 4-5 and 7).

Interestingly, in the presence of trypsin, a 10-fold decrease in the diffusion time from 0.8 ms to 0.08 ms was observed. The latter diffusion time corresponds very strictly to the diffusion time of EGFP alone (V, Fig. 8 A-C). It is clear, that the size of EGFP alone is much smaller than the size of disassembly products by SDS or 6 M urea (Table 6 and 7). This suggests that the fusion moiety is cleaved from the fusion protein by trypsin, and that in the products disassembled from the VLPs by a treatment with 6 M urea or SDS the fusion protein remained intact.

The number of the fusion molecules present in the fluorescent VLPs suggests that the fusion protein in the aminoterminus of VP2 could protrude from the icosahedral 5-fold axis of the capsid. This suggestion results from the presence of 10 fluorescent fusions both in EGFP-VP2 and EGFP-VP40, and 6 units in the construct EGFP-VP23. These numbers show much similarities with studies previously reported for the copy number of VP1 in CPV (Hurtado et al. 1996). In addition, the presence of both the fusion moiety EGFP, as well as the VP2 protein in chimeric VLPs of both B19 and CPV, were validated by FCS (III-V). The number of display units per single VLP, was determined. The results presented in this thesis suggest the possibility of deleting the first 40 amino acids from the VP2 of CPV and utilizing this strategy for designing novel strategies for various display proteins e.g. in targeting of biomolecules (V). Previous studies by Hurtado and co-workers in 1996 made deletion series of constructs of the first 40 amino acids from CPV VP2, and more than 9 residues deletion did not allow VP2 to assemble (Hurtado et al. 1996). Our results, in contrast, show that more than 14 residues deleted again allowed capsid formation. The results presented previously and in this thesis suggest that the first 14 amino acids could be relevant for proper capsid assembly. Additionally our result may suggest that there is a possibility for VP2 to allow better conformation for icosahedral capsid assembly if more than 14 amino acids are removed, since the 40 amino acids could be substituted by EGFP. Thus, by replacing part of the genome 5'-end could still allow natural capsid assembly. Here, EGFP replaces part of the original DNA sequence and the modified VP2 polypeptide can still fold properly to form capsids (V).

It is of great importance that it was possible to calculate the number of non-infectious VLPs displaying EGFP of both B19 (IV, Table 1) as well as CPV (III-V). To our knowledge, this is also the first time when the concentration of non-infectious VLPs displaying EGFP was measured by FCS. Also, previously it

has been demonstrated that transiently expressed EGFP-fusion proteins can be detected by FCS from cellular environments (Brock et al. 1999, Xia et al. 2004). The results in thesis suggests that when the concentration of VLPs is known, more advanced studies for parvoviruses could be achieved such as using these particles as models for studying intracellular trafficking pathways of CPV and B19 by FCS.

Recently, Singh and co-workers showed that even when canine parvovirus was covalently labeled with a fluorescent dye, the virus retained its infectivity (Singh et al. 2006). Thus, viral particles could be used as small cargo nanoboxes for tumor targeting since labeling did not interfere with cellular trafficking. In the present study, VLPs were labeled with EGFP (IV, V). The particles described in this thesis may have several applications e.g. when the intracellular targeting is concerned, since the confocal volume element can be focused inside the cells (Brock & Jovin 1998). However, diffusion inside the cells can be different from that simply monitored *in vitro* in pre-defined buffers. The viscosity inside the cells is different and it is also known that the pH in endosomal (e.g. lysosomes pH 5) (Suikkanen et al. 2003b) vesicles are far from commonly used buffers in FCS (pH 7-8). Following viral trafficking routes by FCS in living cells would, however, require fluorescently labeled virus-like particles or infective viruses. Labeling viral surface molecules may alter specific interactions involved in host cell receptor binding sites and interactions during the transportation within or between cellular compartments. Therefore, virus particles should be labeled without disturbing their natural interactions during infection. This could be performed e.g. by labeling single specific amino acids on the surface. This is difficult, however, due to the large number of identical protein molecules within the viral capsid or envelope. An ideal option could also be to label the interior of the virus-like particle by EGFP and not by display of the fusion partner as described in this thesis (III, IV,V).

7 CONCLUSIONS

Viruses or virus-like particles with or without a display ligand have not been analyzed before by FCS.

Specific conclusions of this study were;

1. The diffusion characteristics of the enveloped virus *Ac*GFPgp64 was determined by FCS. This includes the diffusion coefficient and the hydrodynamic size of the virus. Additionally, the presence, and the number of fluorescent membrane glycoprotein GFPgp64 at the viral membrane was evaluated and verified.

2. The interactions between B19 VLPs of VP2 and antibodies present both in acute-phase as well as in past-immunity serum were detected by FCS. Antibody classes IgM and IgG were distinguished.

3. A study of viral disassembly of both one enveloped and two non-enveloped viral nanoparticles was established by using FCS. Comparisons revealed differences in the size of the formed recombinant fluorescent VLPs, in the number of fusions and in the assembly properties of corresponding VLPs. GFPgp64 fusion proteins at the membrane of the single baculovirus particles were found to contain a minimum of 1.5 disulphide bonds.

4. FCS analysis revealed that the deletion of 14 amino acids from the VP2 amino terminus of CPV prevented VP2 subunits to assemble into VLPs.

Acknowledgements

The work for this thesis began in November 2001, and was primarily processed during the years 2002 to 2005. First of all, I would like to say the greatest of thanks to my supervisors, professor Christian Oker-Blom and professor Matti Vuento. During these years they guided me into the field of research of which I'm indebted and grateful for. Additionally, they also arranged me financial support and moreover, an open-minded and constructive atmosphere to work. We shared many common thoughts on science, or more often, on non-science by a couple of mugs e.g. in Sohwi and Old Brick's. I thank both reviewers, docent Sarah Butcher and professor Erkki Soini for their valuable comments and advice for improvement of this thesis. Special thanks go to Klaus Weisshart of Carl Zeiss. He introduced me to many special "tricks" of FCS, both at the practical, as well as the theoretical level during these years. Special thanks also go to Anna Mäkelä and Leona Gilbert. Thanks to Kirsi Pakkanen, Sanna Kirjavainen, Patrik Michel and Daniel White for their valuable discussions. Moreover, I would like to thank both of our teams, Biochemistry and Biotechnology and the people therein. The idea was to put our strengths together – in the end it's all teamwork. I would like also to pay some attention to my friends. The list would then be too long to be described here in all detail. So, shortly, thanks to Raine, Päiskäri, www.samirintala.com and Iivari. Thanks also to friends Veikkolainen, Rale, Niemelä, Kilppari, Koskimäki and Markus Rantala. Thanks also to my parents and finally, dearest thanks to my girlfriend Eevi. This study was financed in part by Academy of Finland (project # 102161) and the European Union (contract # B10-4CT98-0132). I also want to thank the K.Albin Johansson's Foundation, the Finnish Virology Foundation, the Artturi and Ellen Nyyssönen Foundation, the Instrumentarium Science Foundation and the Ida Montin Foundation for their great financial support.

YHTEENVETO (Résumé in Finnish)

Fluoresenssikorrelaatio-spektroskopia (FCS) on herkkä biofysikaalinen menetelmä, jolla voidaan tutkia makromolekyylien ominaisuuksia vesiliuoksessa. Vaikka menetelmän teoria kehittyi jo 1970–luvun alussa muutaman fyysikon teoretisoinnin tuloksena (Ehrenberg and Rigler 1974, Elson and Madge 1974), kehittyneen laserteknologian ja optiikan ansiosta päästiin vasta 1990-luvun lopulla tutkimaan yksittäisiä biologisia tapahtumia. Sovellutuksia nykylääketieteeseen ollaan vasta kehittämässä. Solussa ja liuoksessa molekyylit liikkuvat satunnaisesti kunnes biomolekyylien väliset elektrostaattiset voimat houkuttelevat ne riittävän lähelle toisiaan ja kiinnittävät kappaleet toisiinsa. FCS:ssä fluoresoivien molekyylien diffuusio liuoksessa tarkasti rajatun lasersäteen läpi aiheuttaa fluoresenssin intensiteetin vaihtelua (Ehrenberg and Rigler 1974, Ehrenberg and Rigler 1976, Madge et al. 1974). Tämä vaihtelu on suhteessa molekyylien mittaustilavuudessa (konfokaalitilavuus ~0.2 femtolitraa) viettämään aikaan ja se on myös suhteessa molekyylien diffuusiovakioon *D*. Diffuusiovakion avulla voidaan laskea makromolekyylin fysikaalinen koko. Mittaamalla riittävän pitkä aika fluoresenssin vaihtelua saadaan molekyylin diffuusiolle tietty keskiarvo. Koska tällöin tiedetään sekä molekyylin diffuusionopeus mittaustilavuuden läpi että mittausaika voidaan laskea toisiinsa vaikuttavien biomolekyylien dissosiaatiovakio.

Tulevaisuudessa FCS-menetelmää voitaneen hyödyntää uusien täsmälääkeainemolekyylien tuotekehityksessä, HTS:ssä (High Throughput Screening), koska tieto ligandin ja kohdemolekyylin interaktiosta saadaan heti sen tapahduttua. Näin säästetään aikaa kalliiden molekyylien seulomisessa.

Tämän väitöskirjan osatutkimuksien (I-V) kohteena olivat ihmisen parvorokkoviruksen B19 (engl. human parvovirus B19), koiran parvoviruksen (CPV, engl. canine parvovirus) viruksen kaltaiset partikkelit (VLP), sekä yksi vaipallinen rakenteellisesti modifioitu bakulovirus. Tutkimuksessa käytetyt VLP:t ovat kooltaan pieniä, halkaisijaltaan 14-20 nm. Tämä koko sopii hyvin fluoresenssikorrelaatio spektroskopiaan. Vaipattomat kohdepartikkelit koostuvat rakenneproteiinista VP2 sekä osassa tapauksissa partikkeleista, joiden VP2:een on geenitekniikan avulla fuusioitu fluoresoiva proteiini, EGFP (engl. enhanced green fluorescence protein). Virusten kaltaiset partikkelit eivät siis sisällä DNA:ta kuten natiivit ja luonnossa itseään kopioivat viruspartikkelit. Turvallisuutensa vuoksi ne sopivat siten hyvin työkaluiksi laboratorioon. Tässä väitöskirjassa tutkittu vaipallinen kohdevirus kuuluu hyönteissoluja infektoivien virusten sukuun, bakuloviruksiin (*Baculoviridae*), ja se sisältää kaksoisjuosteisen DNA –molekyylin. Tämä sauvamainen virus on halkaisijaltaan 25-50 nm ja pituudeltaan 250-300 nm. Koska virus infektoi lähinnä perhosten toukkia, eikä nisäkkäitä, on virus myös turvallinen laboratoriossa. Tutkittavan bakuloviruksen pinnalle on ilmennetty GFP, joka on fuusioitu viruksen omaan vaippaproteiiniin, gp64. Tämä on viruksen genomin koodaama membraaniglykoproteiini, jota virus käyttää hyväkseen tarttuessaan hyönteissolun pinnalle ennen soluun si-

sälle menoa. Tässä väitöskirjassa tutkittiin FCS:llä edellä kuvailtuja viruksen kaltaisia partikkeleita sekä bakulovirusta. Lisäksi yhdessä väitöskirjan osatöistä (II) tarkasteltiin synteettisellä fluorokromilla leimattujen B19 VLP:iden sekä B19-parvorokko-virusinfektion saaneiden potilaiden seerumien vasta-aineiden välistä sitoutumista. Rakenteellisesti modifioitujen virusten kaltaisten nanopartikkeleiden (I, III-V) ja kompleksien (II) kokoa sekä lukumäärää pystyttiin seuraamaan vesiliuoksessa partikkeleiden aiheuttaman lämpöliikkeen ansiosta. VLP:itä sekä fluoresoivaa bakulovirusta käsiteltiin detergenteillä eri pitoisuuksissa. Partikkelit hajosivat liuoksessa jolloin partikkelien lukumäärän ja koon muutos sekä fluoresoivien fuusioproteiinien lukumäärä voitiin todeta FCS:n autokorrelaatiokäyrältä.

REFERENCES

Agbandje, M., S. Kajigaya, R. McKenna, N. S. Young, and M. G. Rossmann. 1994. The structure of human parvovirus B19 at 8 A resolution. Virology 203. 106-115.

Agbandje, M., R. McKenna, M. G. Rossmann, S. Kajigaya, and N. S. Young. 1991. Preliminary X-ray crystallographic investigation of human parvovirus B19. Virology 184. 170-174.

Agbandje, M., R. McKenna, M. G. Rossmann, M. L. Strassheim, and C. R. Parrish. 1993. Structure determination of feline panleukopenia virus empty particles. Proteins 16. 155-171.

Agbandje-McKenna, M., A. L. Llamas-Saiz, F. Wang, P. Tattersall, and M. G. Rossmann. 1998. Functional implications of the structure of the murine parvovirus, minute virus of mice. Structure 6. 1369-1381.

Anderson, M. J., P. G. Higgins, L. R. Davis, J. S. Willman, S. E. Jones, I. M. Kidd, J. R. Pattison, and D. A. Tyrrell. 1985. Experimental parvoviral infection in humans. J Infect Dis 152. 257-265.

Anderson, M. J., E. Lewis, I. M. Kidd, S. M. Hall, and B. J. Cohen. 1984. An outbreak of erythema infectiosum associated with human parvovirus infection. J Hyg (Lond) 93. 85-93.

Arni, R. K., and R. J. Ward. 1996. Phospholipase A2--a structural review. Toxicon 34. 827-841.

Astell, C. R., M. Thomson, M. Merchlinsky, and D. C. Ward. 1983. The complete DNA sequence of minute virus of mice, an autonomous parvovirus. Nucleic Acids Res 11. 999-1018.

Auer, M., K. J. Moore, F. J. Meyer-Almes, R. Guenther, A. J. Pope, and K. A. Stoeckli. 1998. Fluorescence correlation spectroscopy: lead discovery by miniaturized HTS. Drug Discov Today 3. 457-465.

Bacia, K., I. V. Majoul, and P. Schwille. 2002. Probing the endocytic pathway in live cells using dual-color fluorescence cross-correlation analysis. Biophys J 83. 1184-1193.

Bacia, K., and P. Schwille. 2003. A dynamic view of cellular processes by in vivo fluorescence auto- and cross-correlation spectroscopy. Methods 29. 74-85.

Ball-Goodrich, L. J., R. D. Moir, and P. Tattersall. 1991. Parvoviral target cell specificity: acquisition of fibrotropism by a mutant of the lymphotropic strain of minute virus of mice involves multiple amino acid substitutions within the capsid. Virology 184. 175-186.

Bark, N., Z. Foldes-Papp, and R. Rigler. 1999. The incipient stage in thrombin-induced fibrin polymerization detected by FCS at the single molecule level. Biochem Biophys Res Commun 260. 35-41.

Bergeron, J., B. Hebert, and P. Tijssen. 1996. Genome organization of the Kresse strain of porcine parvovirus: identification of the allotropic determinant and comparison with those of NADL-2 and field isolates. J Virol 70. 2508-2515.

Bernacchi, S., G. Mueller, J. Langowski, and W. Waldeck. 2004. Characterization of simian virus 40 on its infectious entry pathway in cells using fluorescence correlation spectroscopy. Biochem Soc Trans 32. 746-749.

Berns, K. I., and S. Adler. 1972. Separation of two types of adeno-associated virus particles containing complementary polynucleotide chains. J Virol 9. 394-396.

Berns, K. I., R. M. Kotin, and M. A. Labow. 1988. Regulation of adeno-associated virus DNA replication. Biochim Biophys Acta 951. 425-429.

Blissard, G. W. 1996. Baculovirus-insect cell interactions. Cytotechnology 20. 73-93.

Blissard, G. W., and G. F. Rohrmann. 1990. Baculovirus diversity and molecular biology. Annu Rev Entomol 35. 127-155.

Boldicke, T., F. Struck, F. Schaper, W. Tegge, H. Sobek, B. Villbrandt, P. Lankenau, and M. Bocher. 2000. A new peptide-affinity tag for the detection and affinity purification of recombinant proteins with a monoclonal antibody. J Immunol Methods 240. 165-183.

Boonen, G., A. Pramanik, R. Rigler, and H. Haberlein. 2000. Evidence for specific interactions between kavain and human cortical neurons monitored by fluorescence correlation spectroscopy. Planta Med 66. 7-10.

Bouchaud, J. P., and A. Georges. 1990. Comment on "Stochastic pathway to anomalous diffusion". Phys Rev A 41. 1156-1157.

Boyce, F. M., and N. L. Bucher. 1996. Baculovirus-mediated gene transfer into mammalian cells. Proc Natl Acad Sci U S A 93. 2348-2352.

Brock, R., and T. M. Jovin. 1998. Fluorescence correlation microscopy (FCM)-fluorescence correlation spectroscopy (FCS) taken into the cell. Cell Mol Biol 44. 847-856.

Brock, R., G. Vamosi, G. Vereb, and T. M. Jovin. 1999. Rapid characterization of green fluorescent protein fusion proteins on the molecular and cellular level by fluorescence correlation microscopy. Proc Natl Acad Sci U S A 96. 10123-10128.

Brown, C. S., T. Jensen, R. H. Meloen, W. Puijk, K. Sugamura, H. Sato, and W. J. Spaan. 1992. Localization of an immunodominant domain on baculovirus-produced parvovirus B19 capsids: correlation to a major surface region on the native virus particle. J Virol 66. 6989-6996.

Brown, C. S., J. W. Van Lent, J. M. Vlak, and W. J. Spaan. 1991. Assembly of empty capsids by using baculovirus recombinants expressing human parvovirus B19 structural proteins. J Virol 65. 2702-2706.

Brown, C. S., S. Welling-Wester, M. Feijlbrief, J. W. Van Lent, and W. J. Spaan. 1994. Chimeric parvovirus B19 capsids for the presentation of foreign epitopes. Virology 198. 477-488.

Brown, K. E., S. M. Anderson, and N. S. Young. 1993. Erythrocyte P antigen: cellular receptor for B19 parvovirus. Science 262. 114-117.

Burgess, S. 1977. Molecular weights of lepidopteran baculovirus DNAs: Derivation by electron microscopy. J Gen Virol 37. 501-510.

Busschots, K., J. Vercammen, S. Emiliani, R. Benarous, Y. Engelborghs, F. Christ, and Z. Debyser. 2005. The interaction of LEDGF/p75 with integrase is lentivirus-specific and promotes DNA binding. J Biol Chem 280. 17841-17847.

Carreira, A., M. Menendez, J. Reguera, J. M. Almendral, and M. G. Mateu. 2004. In vitro disassembly of a parvovirus capsid and effect on capsid stability of heterologous peptide insertions in surface loops. J Biol Chem 279. 6517-6525.

Caspar, D. L., and A. Klug. 1962. Physical principles in the construction of regular viruses. Cold Spring Harb Symp Quant Biol 27. 1-24.

Cassinotti, P., G. Siegl, B. A. Michel, and P. Bruhlmann. 1998. Presence and significance of human parvovirus B19 DNA in synovial membranes and bone marrow from patients with arthritis of unknown origin. J Med Virol 56. 199-204.

Chapman, M. S., and M. G. Rossmann. 1993. Structure, sequence, and function correlations among parvoviruses. Virology 194. 491-508.

Charpilienne, A., M. Nejmeddine, M. Berois, N. Parez, E. Neumann, E. Hewat, G. Trugnan, and J. Cohen. 2001. Individual rotavirus-like particles containing 120 molecules of fluorescent protein are visible in living cells. J Biol Chem 276. 29361-29367.

Chattopadhyay, K., E. L. Elson, and C. Frieden. 2005. The kinetics of conformational fluctuations in an unfolded protein measured by fluorescence methods. Proc Natl Acad Sci U S A 102. 2385-2389.

Chattopadhyay, K., S. Saffarian, E. L. Elson, and C. Frieden. 2002. Measurement of microsecond dynamic motion in the intestinal fatty acid binding protein by using fluorescence correlation spectroscopy. Proc Natl Acad Sci U S A 99. 14171-14176.

Chen, Y., J. D. Muller, K. M. Berland, and E. Gratton. 1999. Fluorescence fluctuation spectroscopy. Methods 19. 234-252.

Christensen, J., T. Storgaard, B. Bloch, S. Alexandersen, and B. Aasted. 1993. Expression of Aleutian mink disease parvovirus proteins in a baculovirus vector system. J Virol 67. 229-238.

Christensen, J., and P. Tattersall. 2002. Parvovirus initiator protein NS1 and RPA coordinate replication fork progression in a reconstituted DNA replication system. J Virol 76. 6518-6531.

Corsini, J., J. O. Carlson, F. Maxwell, and I. H. Maxwell. 1995. Symmetric-strand packaging of recombinant parvovirus LuIII genomes that retain only the terminal regions. J Virol 69. 2692-2696.

Cossart, Y. E., A. M. Field, B. Cant, and D. Widdows. 1975. Parvovirus-like particles in human sera. Lancet 1. 72-73.

Cotmore, S. F., M. Gunther, and P. Tattersall. 1989. Evidence for a ligation step in the DNA replication of the autonomous parvovirus minute virus of mice. J Virol 63. 1002-1006.

Cotmore, S. F., and P. Tattersall. 1984. Characterization and molecular cloning of a human parvovirus genome. Science 226. 1161-1165.

Cotmore, S. F., and P. Tattersall. 1986. Organization of nonstructural genes of the autonomous parvovirus minute virus of mice. J Virol 58. 724-732.

Cotmore, S. F., and P. Tattersall. 1987. The autonomously replicating parvoviruses of vertebrates. Adv Virus Res 33. 91-174.

Cotmore, S. F., and P. Tattersall. 1992. In vivo resolution of circular plasmids containing concatemer junction fragments from minute virus of mice DNA and their subsequent replication as linear molecules. J Virol 66. 420-431.

Cotmore, S. F., and P. Tattersall. 2005. Encapsidation of minute virus of mice DNA: aspects of the translocation mechanism revealed by the structure of partially packaged genomes. Virology 336. 100-112.

Crawford, L. V. 1966. A minute virus of mice. Virology 29. 605-612.

Damodaran, K. V., V. S. Reddy, Johnson, J. E.,, and C. L. Brooks. 2002. A General Method to Quantify Quasi-equivalence in Icosahedral Viruses. J Mol Biol 324. 723–737.

Dorsch, S., G. Liebisch, B. Kaufmann, P. von Landenberg, J. H. Hoffmann, W. Drobnik, and S. Modrow. 2002. The VP1 unique region of parvovirus B19 and its constituent phospholipase A2-like activity. J Virol 76. 2014-2018.

Ehrenberg, M., and R. Rigler. 1974. Rotational Brownian motion and fluorescence intensity fluctuations. Chem Phys 4. 390-401.

Ehrenberg, M., and R. Rigler. 1976. Fluorescence correlation spectroscopy applied to rotational diffusion of macromolecules. Q Rev Biophys 9. 69-81.

Eigen, M., and R. Rigler. 1994. Sorting single molecules: application to diagnostics and evolutionary biotechnology. Proc Natl Acad Sci U S A 91. 5740-5747.

Elson, E. L. 2001. Fluorescence correlation spectroscopy measures molecular transport in cells. Traffic 2. 789-796.

Elson, E. L., and D. Madge. 1974. Fluorescence correlation spectroscopy. I. Conceptual basis and theory. Biopolymers 13. 1-27.

Ernst, W. J., A. Spenger, L. Toellner, H. Katinger, and R. M. Grabherr. 2000. Expanding baculovirus surface display. Modification of the native coat protein gp64 of Autographa californica NPV. Eur J Biochem 267. 4033-4039.

Flipsen, J. T., R. M. Mans, A. W. Kleefsman, D. Knebel-Morsdorf, and J. M. Vlak. 1995. Deletion of the baculovirus ecdysteroid UDP-glucosyltransferase gene induces early degeneration of Malpighian tubules in infected insects. J Virol 69. 4529-4532.

Foldes-Papp, Z., B. Angerer, P. Thyberg, M. Hinz, S. Wennmalm, W. Ankenbauer, H. Seliger, A. Holmgren, and R. Rigler. 2001a. Fluorescently labeled model DNA sequences for exonucleolytic sequencing. J Biotechnol 86. 203-224.

Foldes-Papp, Z., U. Demel, and G. P. Tilz. 2001b. Ultrasensitive detection and identification of fluorescent molecules by FCS: impact for immunobiology. Proc Natl Acad Sci U S A 98. 11509-11514.

Foldes-Papp, Z., U. Demel, and G. P. Tilz. 2002. Detection of single molecules: solution-phase single-molecule fluorescence correlation spectroscopy as an ultrasensitive, rapid and reliable system for immunological investigation. J Immunol Methods 260. 117-124.

Foldes-Papp, Z., and R. Rigler. 2001. Quantitative two-color fluorescence cross-correlation spectroscopy in the analysis of polymerase chain reaction. Biol Chem 382. 473-478.

Foquet, M., J. Korlach, W. Zipfel, W. W. Webb, and H. G. Craighead. 2002. DNA fragment sizing by single molecule detection in submicrometer-sized closed fluidic channels. Anal Chem 74. 1415-1422.

Fradin, C., A. Abu-Arish, R. Granek, and M. Elbaum. 2003. Fluorescence correlation spectroscopy close to a fluctuating membrane. Biophys J 84. 2005-2020.

Franssila, R., and K. Hedman. 2004. T-helper cell-mediated interferon-gamma, interleukin-10 and proliferation responses to a candidate recombinant vaccine for human parvovirus B19. Vaccine 22. 3809-3815.

Fraser, M. J. 1986. Ultrastructural observations of virion maturation in Autographa californica nuclear polyhedrosis virus infected Spodoptera frugiperda cell cultures. J Ultrastruct Mol Struct Res 95. 189-195.

Frickhofen, N., and N. S. Young. 1989. Persistent parvovirus B19 infections in humans. Microb Pathog 7. 319-327.

Friesen, P. D., and L. K. Miller. 2001. Insect viruses. D. M. Knipe, P. M. Howley, and D. E. Griffin, (Eds). Fields Virology, Vol. 1. Lippincott Williams & Wilkins, PA, USA., 599-628.

Gardiner, E. M., and P. Tattersall. 1988. Evidence that developmentally regulated control of gene expression by a parvoviral allotropic determinant is particle mediated. J Virol 62. 1713-1722.

Gilbert, L., J. Toivola, E. Lehtomaki, L. Donaldson, P. Kapyla, M. Vuento, and C. Oker-Blom. 2004. Assembly of fluorescent chimeric virus-like particles of canine parvovirus in insect cells. Biochem Biophys Res Commun 313. 878-887.

Gosch, M., and R. Rigler. 2005. Fluorescence correlation spectroscopy of molecular motions and kinetics. Adv Drug Deliv Rev 57. 169-190.

Grabherr, R., W. Ernst, O. Doblhoff-Dier, M. Sara, and H. Katinger. 1997. Expression of foreign proteins on the surface of Autographa californica nuclear polyhedrosis virus. Biotechniques 22. 730-735.

Grabherr, R., W. Ernst, C. Oker-Blom, and I. Jones. 2001. Developments in the use of baculoviruses for the surface display of complex eukaryotic proteins. Trends Biotechnol 19. 231-236.

Greber, U. F. 2002. Signalling in viral entry. Cell Mol Life Sci 59. 608-626.

Haas-Stapleton, E. J., J. O. Washburn, and L. E. Volkman. 2004. P74 mediates specific binding of Autographa californica M nucleopolyhedrovirus occlusion-derived virus to primary cellular targets in the midgut epithelia of Heliothis virescens Larvae. J Virol 78. 6786-6791.

Hartig, G. R., T. T. Tran, and M. L. Smythe. 2005. Intramolecular disulphide bond arrangements in nonhomologous proteins. Protein Sci 14. 474-482.

Haupts, U., S. Maiti, P. Schwille, and W. W. Webb. 1998. Dynamics of fluorescence fluctuations in green fluorescent protein observed by fluorescence correlation spectroscopy. Proc Natl Acad Sci U S A 95. 13573-13578.

Hefferon, K. L., A. G. Oomens, S. A. Monsma, C. M. Finnerty, and G. W. Blissard. 1999. Host cell receptor binding by baculovirus GP64 and kinetics of virion entry. Virology 258. 455-468.

Hegener, O., R. Jordan, and H. Haberlein. 2002. Benzodiazepine binding studies on living cells: application of small ligands for fluorescence correlation spectroscopy. Biol Chem 383. 1801-1807.

Henriksson, M., A. Pramanik, J. Shafqat, Z. Zhong, M. Tally, K. Ekberg, J. Wahren, R. Rigler, J. Johansson, and H. Jornvall. 2001. Specific Binding of Proinsulin C-Peptide to Intact and to Detergent-Solubilized Human Skin Fibroblasts*1. Biochem Biophys Res Commun 280. 423-427.

Hermonat, P. L., M. A. Labow, R. Wright, K. I. Berns, and N. Muzyczka. 1984. Genetics of adeno-associated virus: isolation and preliminary characterization of adeno-associated virus type 2 mutants. J Virol 51. 329-339.

Hernando, E., A. L. Llamas-Saiz, C. Foces-Foces, R. McKenna, I. Portman, M. Agbandje-McKenna, and J. M. Almendral. 2000. Biochemical and physical characterization of parvovirus minute virus of mice virus-like particles. Virology 267. 299-309.

Hollister, J., H. Conradt, and D. L. Jarvis. 2003. Evidence for a sialic acid salvaging pathway in lepidopteran insect cells. Glycobiology 13. 487-495.

Hollister, J. R., and D. L. Jarvis. 2001. Engineering lepidopteran insect cells for sialoglycoprotein production by genetic transformation with mammalian beta 1,4-galactosyltransferase and alpha 2,6-sialyltransferase genes. Glycobiology 11. 1-9.

Hollister, J. R., J. H. Shaper, and D. L. Jarvis. 1998. Stable expression of mammalian beta 1,4-galactosyltransferase extends the N-glycosylation pathway in insect cells. Glycobiology 8. 473-480.

Hoque, M., N. Shimizu, K. Ishizu, H. Yajima, F. Arisaka, K. Suzuki, H. Watanabe, and H. Handa. 1999. Chimeric virus-like particle formation of adeno-associated virus. Biochem Biophys Res Commun 266. 371-376.

Horiuchi, M., N. Ishiguro, H. Goto, and M. Shinagawa. 1992. Characterization of the stage(s) in the virus replication cycle at which the host-cell specificity of the feline parvovirus subgroup is regulated in canine cells. Virology 189. 600-608.

Huijskens, I., L. Li, L. G. Willis, and D. A. Theilmann. 2004. Role of AcMNPV IE0 in baculovirus very late gene activation. Virology 323. 120-130.

Hurtado, A., P. Rueda, J. Nowicky, J. Sarraseca, and J. Casal. 1996. Identification of domains in canine parvovirus VP2 essential for the assembly of virus-like particles. J Virol 70. 5422-5429.

Issaeva, N., P. Bozko, M. Enge, M. Protopopova, L. G. Verhoef, M. Masucci, A. Pramanik, and G. Selivanova. 2004. Small molecule RITA binds to p53, blocks p53-HDM-2 interaction and activates p53 function in tumors. Nat Med 10. 1321-1328.

Jermutus, L., R. Kolly, Z. Foldes-Papp, J. Hanes, R. Rigler, and A. Pluckthun. 2002. Ligand binding of a ribosome-displayed protein detected in solution at the single molecule level by fluorescence correlation spectroscopy. Eur Biophys J 31. 179-184.

Kaba, S. A., J. C. Hemmes, J. W. van Lent, J. M. Vlak, V. Nene, A. J. Musoke, and M. M. van Oers. 2003. Baculovirus surface display of Theileria parva p67 antigen preserves the conformation of sporozoite-neutralizing epitopes. Protein Eng 16. 73-78.

Kaikkonen, L., H. Lankinen, I. Harjunpaa, K. Hokynar, M. Soderlund-Venermo, C. Oker-Blom, L. Hedman, and K. Hedman. 1999. Acute-phase-specific heptapeptide epitope for diagnosis of parvovirus B19 infection. J Clin Microbiol 37. 3952-3956.

Kajigaya, S., H. Fujii, A. Field, S. Anderson, S. Rosenfeld, L. J. Anderson, T. Shimada, and N. S. Young. 1991. Self-assembled B19 parvovirus capsids, produced in a baculovirus system, are antigenically and immunogenically similar to native virions. Proc Natl Acad Sci U S A 88. 4646-4650.

Kask, P., K. Palo, N. Fay, L. Brand, U. Mets, D. Ullmann, J. Jungmann, J. Pschorr, and K. Gall. 2000. Two-dimensional fluorescence intensity distribution analysis: theory and applications. Biophys J 78. 1703-1713.

Katta, R. 2002. Parvovirus B19: a review. Dermatol Clin 20. 333-342.

Kawase, M., M. Momoeda, N. S. Young, and S. Kajigaya. 1995. Modest truncation of the major capsid protein abrogates B19 parvovirus capsid formation. J Virol 69. 6567-6571.

Kost, T. A., J. P. Condreay, and D. L. Jarvis. 2005. Baculovirus as versatile vectors for protein expression in insect and mammalian cells. Nat Biotechnol 23. 567-575.

Kukkonen, S. P., K. J. Airenne, V. Marjomaki, O. H. Laitinen, P. Lehtolainen, P. Kankaanpaa, A. J. Mahonen, J. K. Raty, H. R. Nordlund, C. Oker-Blom, M. S. Kulomaa, and S. Yla-Herttuala. 2003. Baculovirus capsid display: a novel tool for transduction imaging. Mol Ther 8. 853-862.

Laemmli, U. K. 1970. Cleavage of structural proteins during the assembly of the head of bacteriophage T4. Nature 227. 680-685.

Lamb, D. C., A. Schenk, C. Rocker, C. Scalfi-Happ, and G. U. Nienhaus. 2000. Sensitivity enhancement in fluorescence correlation spectroscopy of multiple species using time-gated detection. Biophys J 79. 1129-1138.

Legrand, C., J. Rommelaere, and P. Caillet-Fauquet. 1993. MVM(p) NS-2 protein expression is required with NS-1 for maximal cytotoxicity in human transformed cells. Virology 195. 149-155.

Leng, X., K. Startchev, and J. Buffle. 2002. Application of Fluorescence Correlation Spectroscopy: A Study of Flocculation of Rigid Rod-like

Biopolymer (Schizophyllan) and Colloidal Particles. J Colloid Interf Sci 251. 64-72.

Liang, C., J. Song, and X. Chen. 2005. The GP64 protein of Autographa californica multiple nucleopolyhedrovirus rescues Helicoverpa armigera nucleopolyhedrovirus transduction in mammalian cells. J Gen Virol 86. 1629-1635.

Lindley, K. M., J. L. Su, P. K. Hodges, G. B. Wisely, R. K. Bledsoe, J. P. Condreay, D. A. Winegar, J. T. Hutchins, and T. A. Kost. 2000. Production of monoclonal antibodies using recombinant baculovirus displaying gp64-fusion proteins. J Immunol Methods 234. 123-135.

Llamas-Saiz, A. L., M. Agbandje-McKenna, W. R. Wikoff, J. Bratton, P. Tattersall, and M. G. Rossmann. 1997. Structure determination of minute virus of mice. Acta Crystallogr D Biol Crystallogr 53. 93-102.

Lombardo, E., J. C. Ramirez, M. Agbandje-McKenna, and J. M. Almendral. 2000. A beta-stranded motif drives capsid protein oligomers of the parvovirus minute virus of mice into the nucleus for viral assembly. J Virol 74. 3804-3814.

Lux, K., N. Goerlitz, S. Schlemminger, L. Perabo, D. Goldnau, J. Endell, K. Leike, D. M. Kofler, S. Finke, M. Hallek, and H. Buning. 2005. Green fluorescent protein-tagged adeno-associated virus particles allow the study of cytosolic and nuclear trafficking. J Virol 79. 11776-11787.

Madge, D., E. L. Elson, and W. W. Webb. 1974. Fluorescence correlation spectroscopy. II. An experimental realization. Biopolymers 13. 29-61.

Maeda, H., H. Shimokawa, S. Satoh, H. Nakano, and T. Nunoue. 1988. Nonimmunologic hydrops fetalis resulting from intrauterine human parvovirus B-19 infection: report of two cases. Obstet Gynecol 72. 482-485.

Maertens, G., J. Vercammen, Z. Debyser, and Y. Engelborghs. 2005. Measuring protein-protein interactions inside living cells using single color fluorescence correlation spectroscopy. Application to human immunodeficiency virus type 1 integrase and LEDGF/p75. Faseb J 19. 1039-1041.

Maiti, S., U. Haupts, and W. W. Webb. 1997. Fluorescence correlation spectroscopy: diagnostics for sparse molecules. Proc Natl Acad Sci U S A 94. 11753-11757.

Marchal, I., M. Cerutti, A. M. Mir, S. Juliant, G. Devauchelle, R. Cacan, and A. Verbert. 2001. Expression of a membrane-bound form of Trypanosoma cruzi trans-sialidase in baculovirus-infected insect cells: a potential tool for sialylation of glycoproteins produced in the baculovirus-insect cells system. Glycobiology 11. 593-603.

Margittai, M., J. Widengren, E. Schweinberger, G. F. Schroder, S. Felekyan, E. Haustein, M. Konig, D. Fasshauer, H. Grubmuller, R. Jahn, and C. A. Seidel. 2003. Single-molecule fluorescence resonance energy transfer reveals a dynamic equilibrium between closed and open conformations of syntaxin 1. Proc Natl Acad Sci U S A 100. 15516-15521.

Marheineke, K., S. Grunewald, W. Christie, and H. Reilander. 1998. Lipid composition of Spodoptera frugiperda (Sf9) and Trichoplusia ni (Tn) insect cells used for baculovirus infection. FEBS Lett 441. 49-52.

Markovic, I., H. Pulyaeva, A. Sokoloff, and L. V. Chernomordik. 1998. Membrane fusion mediated by baculovirus gp64 involves assembly of stable gp64 trimers into multiprotein aggregates. J Cell Biol 143. 1155-1166.

Marquardt, D. 1963. An algorithm for least-squares estimation of nonlinear parameters. J Soc Indust Appl Math 11. 431-441.

Masuda, A., K. Ushida, and T. Okamoto. 2005. New fluorescence correlation spectroscopy enabling direct observation of spatiotemporal dependence of diffusion constants as an evidence of anomalous transport in extracellular matrices. Biophys J 88. 3584-3591.

Meissner, O., and H. Haberlein. 2003. Lateral mobility and specific binding to GABA(A) receptors on hippocampal neurons monitored by fluorescence correlation spectroscopy. Biochemistry 42. 1667-1672.

Meneses, P., K. I. Berns, and E. Winocour. 2000. DNA sequence motifs which direct adeno-associated virus site-specific integration in a model system. J Virol 74. 6213-6216.

Meseth, U., T. Wohland, R. Rigler, and H. Vogel. 1999. Resolution of fluorescence correlation measurements. Biophys J 76. 1619-1631.

Meyer-Almes, F. J., and M. Auer. 2000. Enzyme inhibition assays using fluorescence correlation spectroscopy: a new algorithm for the derivation of kcat/KM and Ki values at substrate concentrations much lower than the Michaelis constant. Biochemistry 39. 13261-13268.

Meyer-Almes, F.-J., K. Wyzgol, and M. J. Powell. 1998. Mechanism of the [alpha]-complementation reaction of E. coli [beta]-galactosidase deduced from fluorescence correlation spectroscopy measurements. Biophys Chem 75. 151-160.

Michel, P. 2002. Expression, Purification and Characterization of Human Parvovirus B19 Virus-Like Particles. Pages 92. *Department of Biological and Environmental Science*. University of Jyväskylä, Jyväskylä.

Miller, L. K. 1988. Baculoviruses as gene expression vectors. Annu Rev Microbiol 42. 177-199.

Moore, T. L. 2000. Parvovirus-associated arthritis. Curr Opin Rheumatol 12. 289-294.

Mottershead, D., I. van der Linden, C. H. von Bonsdorff, K. Keinanen, and C. Oker-Blom. 1997. Baculoviral display of the green fluorescent protein and rubella virus envelope proteins. Biochem Biophys Res Commun 238. 717-722.

Myers, M. W., and B. J. Carter. 1980. Assembly of adeno-associated virus. Virology 102. 71-82.

Naides, S. J., Y. V. Karetnyi, L. L. Cooling, R. S. Mark, and A. N. Langnas. 1996. Human parvovirus B19 infection and hepatitis. Lancet 347. 1563-1564.

Oehlenschlager, F., P. Schwille, and M. Eigen. 1996. Detection of HIV-1 RNA by nucleic acid sequence-based amplification combined with fluorescence correlation spectroscopy. Proc Natl Acad Sci U S A 93. 12811-12816.

Ojala, K., J. Koski, W. Ernst, R. Grabherr, I. Jones, and C. Oker-Blom. 2004. Improved display of synthetic IgG-binding domains on the baculovirus surface. Technol Cancer Res Treat 3. 77-84.

Ojala, K., D. G. Mottershead, A. Suokko, and C. Oker-Blom. 2001. Specific binding of baculoviruses displaying gp64 fusion proteins to mammalian cells. Biochem Biophys Res Commun 284. 777-784.

Oker-Blom, C., K. J. Airenne, and R. Grabherr. 2003. Baculovirus display strategies: Emerging tools for eukaryotic libraries and gene delivery. Brief Funct Genomic Proteomic 2. 244-253.

Olszewski, J., and L. K. Miller. 1997. Identification and characterization of a baculovirus structural protein, VP1054, required for nucleocapsid formation. J Virol 71. 5040-5050.

Oomens, A. G., and G. W. Blissard. 1999. Requirement for GP64 to drive efficient budding of Autographa californica multicapsid nucleopolyhedrovirus. Virology 254. 297-314.

O'Reilly, D. R., L. K. Miller, and V. A. Lucknow. 1992. Baculovirus Expression Vector. A Laboratory Manual, Vol. W. H. Freeman and Co, New York,

Pamidi, S., K. Friedman, B. Kampalath, C. Eshoa, and S. Hariharan. 2000. Human parvovirus B19 infection presenting as persistent anemia in renal transplant recipients. Transplantation 69. 2666-2669.

Pardi, D. S., Y. Romero, L. E. Mertz, and D. D. Douglas. 1998. Hepatitis-associated aplastic anemia and acute parvovirus B19 infection: a report of two cases and a review of the literature. Am J Gastroenterol 93. 468-470.

Parker, J. S., W. J. Murphy, D. Wang, S. J. O'Brien, and C. R. Parrish. 2001. Canine and feline parvoviruses can use human or feline transferrin receptors to bind, enter, and infect cells. J Virol 75. 3896-3902.

Parker, J. S., and C. R. Parrish. 1997. Canine parvovirus host range is determined by the specific conformation of an additional region of the capsid. J Virol 71. 9214-9222.

Parker, J. S., and C. R. Parrish. 2000. Cellular uptake and infection by canine parvovirus involves rapid dynamin-regulated clathrin-mediated endocytosis, followed by slower intracellular trafficking. J Virol 74. 1919-1930.

Parrish, C. R. 1991. Mapping specific functions in the capsid structure of canine parvovirus and feline panleukopenia virus using infectious plasmid clones. Virology 183. 195-205.

Parrish, C. R., L. E. Carmichael, and D. F. Antczak. 1982. Antigenic relationships between canine parvovirus type 2, feline panleukopenia virus and mink enteritis virus using conventional antisera and monoclonal antibodies. Arch Virol 72. 267-278.

Pintel, D., D. Dadachanji, C. R. Astell, and D. C. Ward. 1983. The genome of minute virus of mice, an autonomous parvovirus, encodes two overlapping transcription units. Nucleic Acids Res 11. 1019-1038.

Pitschke, M., R. Prior, M. Haupt, and D. Riesner. 1998. Detection of single amyloid beta-protein aggregates in the cerebrospinal fluid of Alzheimer's patients by fluorescence correlation spectroscopy. Nat Med 4. 832-834.

Pramanik, A. 2004. Ligand-receptor interactions in live cells by fluorescence correlation spectroscopy. Curr Pharm Biotechnol 5. 205-212.

Pramanik, A., K. Ekberg, Z. Zhong, J. Shafqat, M. Henriksson, O. Jansson, A. Tibell, M. Tally, J. Wahren, and a. Jornvall et. 2001. C-peptide binding to human cell membranes: importance of Glu27. Biochem Biophys Res Commun 284. 94-98.

Pramanik, A., and R. Rigler. 2001. Ligand-receptor interactions in the membrane of cultured cells monitored by fluorescence correlation spectroscopy. Biol Chem 382. 371-378.

Pramanik, A., and J. Widengren. 2004. Fluorescence correlation spectroscopy (FCS). R. A. Meyers, ed. Encyclopedia of Molecular Cell Biology and Molecular Medicine, Vol. Willey-VCH, 461-500.

Rauer, B., E. Neumann, J. Widengren, and R. Rigler. 1996. Fluorescence correlation spectrometry of the interaction kinetics of tetramethylrhodamin [alpha]-bungarotoxin with Torpedo californica acetylcholine receptor. Biophys Chem 58. 3-12.

Reguera, J., A. Carreira, L. Riolobos, J. M. Almendral, and M. G. Mateu. 2004. Role of interfacial amino acid residues in assembly, stability, and conformation of a spherical virus capsid. Proc Natl Acad Sci U S A 101. 2724-2729.

Reznikov, K., L. Kolesnikova, A. Pramanik, K. Tan-No, I. Gileva, T. Yakovleva, R. Rigler, L. Terenius, and G. Bakalkin. 2000. Clustering of apoptotic cells via bystander killing by peroxides. Faseb J 14. 1754-1764.

Rhode, S. L., 3rd. 1985a. Nucleotide sequence of the coat protein gene of canine parvovirus. J Virol 54. 630-633.

Rhode, S. L., 3rd. 1985b. trans-Activation of parvovirus P38 promoter by the 76K noncapsid protein. J Virol 55. 886-889.

Rhode, S. L., 3rd. 1989. Both excision and replication of cloned autonomous parvovirus DNA require the NS1 (rep) protein. J Virol 63. 4249-4256.

Rhode, S. L., 3rd, and S. M. Richard. 1987. Characterization of the trans-activation-responsive element of the parvovirus H-1 P38 promoter. J Virol 61. 2807-2815.

Richards, R., P. Linser, and R. W. Armentrout. 1977. Kinetics of assembly of a parvovirus, minute virus of mice, in synchronized rat brain cells. J Virol 22. 778-793.

Rigler, R. 1995. Fluorescence correlations, single molecule detection and large number screening. Applications in biotechnology. J Biotechnol 41. 177-186.

Rigler, R., and E. L. Elson. 2001. *Fluorescence Correlation Spectroscopy (FCS). Theory and Applications*. Springer-Verlag, Berlin Heidelberg, Berlin, Heidelberg.

Rigler, R., Z. Foldes-Papp, F. J. Meyer-Almes, C. Sammet, M. Volcker, and A. Schnetz. 1998. Fluorescence cross-correlation: a new concept for polymerase chain reaction. J Biotechnol 63. 97-109.

Rigler, R., Ü. Mets, J. Widengren, and P. Kask. 1993. Fluorescence correlation spectroscopy with high count rate and low background: analysis of translational diffusion. Eur Biophys J 22. 169-175.

Rigler, R., A. Pramanik, P. Jonasson, G. Kratz, O. T. Jansson, P. Nygren, S. Stahl, K. Ekberg, B. Johansson, and a. Uhlen et. 1999. Specific binding of proinsulin C-peptide to human cell membranes. Proc Natl Acad Sci U S A 96. 13318-13323.

Rigler, R., and J. Widengren. 1990. Ultrasensitive detection of single molecules by fluorescence correlation spectroscopy. Bioscience 3. 180-183.

Riikonen, R., H. Matilainen, N. Rajala, O. Pentikainen, M. Johnson, J. Heino, and C. Oker-Blom. 2005. Functional display of an alpha2 integrin-specific motif (RKK) on the surface of baculovirus particles. Technol Cancer Res Treat 4. 437-445.

Rodis, J. F., T. J. Hovick, Jr., D. L. Quinn, S. S. Rosengren, and P. Tattersall. 1988. Human parvovirus infection in pregnancy. Obstet Gynecol 72. 733-738.

Rohrmann, G. F. 1986. Polyhedrin structure. J Gen Virol 67 (Pt 8). 1499-1513.

Rose, J. A., J. V. Maizel, Jr., J. K. Inman, and A. J. Shatkin. 1971. Structural proteins of adenovirus-associated viruses. J Virol 8. 766-770.

Rosenfeld, S. J., K. Yoshimoto, S. Kajigaya, S. Anderson, N. S. Young, A. Field, P. Warrener, G. Bansal, and M. S. Collett. 1992. Unique region of the minor capsid protein of human parvovirus B19 is exposed on the virion surface. J Clin Invest 89. 2023-2029.

Roy, P. 1996. Multiple gene expression in baculovirus system. Third generation vaccines for bluetongue disease and African horsesickness disease. Ann N Y Acad Sci 791. 318-332.

Ruffing, M., H. Zentgraf, and J. A. Kleinschmidt. 1992. Assembly of viruslike particles by recombinant structural proteins of adeno-associated virus type 2 in insect cells. J Virol 66. 6922-6930.

Saliki, J. T., B. Mizak, H. P. Flore, R. R. Gettig, J. P. Burand, L. E. Carmichael, H. A. Wood, and C. R. Parrish. 1992. Canine parvovirus empty capsids produced by expression in a baculovirus vector: use in analysis of viral properties and immunization of dogs. J Gen Virol 73 (Pt 2). 369-374.

Saxton, M. J. 1996. Anomalous diffusion due to binding: a Monte Carlo study. Biophys J 70. 1250-1262.

Schwille, P., J. Bieschke, and F. Oehlenschlager. 1997a. Kinetic investigations by fluorescence correlation spectroscopy: the analytical and diagnostic potential of diffusion studies. Biophys Chem 66. 211-228.

Schwille, P., U. Haupts, S. Maiti, and W. W. Webb. 1999a. Molecular dynamics in living cells observed by fluorescence correlation spectroscopy with one- and two-photon excitation. Biophys J 77. 2251-2265.

Schwille, P., and U. Kettling. 2001. Analyzing single protein molecules using optical methods. Curr Opin Biotech 12. 382-386.

Schwille, P., J. Korlach, and W. W. Webb. 1999b. Fluorescence correlation spectroscopy with single-molecule sensitivity on cell and model membranes. Cytometry 36. 176-182.

Schwille, P., F. J. Meyer-Almes, and R. Rigler. 1997b. Dual-color fluorescence cross-correlation spectroscopy for multicomponent diffusional analysis in solution. Biophys J 72. 1878-1886.

Senapathy, P., J. D. Tratschin, and B. J. Carter. 1984. Replication of adeno-associated virus DNA. Complementation of naturally occurring rep-mutants by a wild-type genome or an ori- mutant and correction of terminal palindrome deletions. J Mol Biol 179. 1-20.

Shade, R. O., M. C. Blundell, S. F. Cotmore, P. Tattersall, and C. R. Astell. 1986. Nucleotide sequence and genome organization of human parvovirus B19 isolated from the serum of a child during aplastic crisis. J Virol 58. 921-936.

Siegel, G., R. C. Bates, K. I. Berns, B. J. Carter, D. C. Kelly, E. Kurstak, and P. Tattersall. 1985. Characteristics and taxonomy of parvoviridae. Intervirology 23. 61-73.

Singh, P., G. Destito, A. Schneemann, and M. Manchester. 2006. Canine parvovirus-like particles, a novel nanomaterial for tumor targeting. J Nanobiotechnology 4. 2.

Smith, A. E., and A. Helenius. 2004. How viruses enter animal cells. Science 304. 237-242.

Suikkanen, S., T. Aaltonen, M. Nevalainen, O. Valilehto, L. Lindholm, M. Vuento, and M. Vihinen-Ranta. 2003a. Exploitation of microtubule cytoskeleton and dynein during parvoviral traffic toward the nucleus. J Virol 77. 10270-10279.

Suikkanen, S., M. Antila, A. Jaatinen, M. Vihinen-Ranta, and M. Vuento. 2003b. Release of canine parvovirus from endocytic vesicles. Virology 316. 267-280.

Suikkanen, S., K. Saajarvi, J. Hirsimaki, O. Valilehto, H. Reunanen, M. Vihinen-Ranta, and M. Vuento. 2002. Role of recycling endosomes and lysosomes in dynein-dependent entry of canine parvovirus. J Virol 76. 4401-4411.

Summerford, C., J. S. Bartlett, and R. J. Samulski. 1999. AlphaVbeta5 integrin: a co-receptor for adeno-associated virus type 2 infection. Nat Med 5. 78-82.

Summers, J., S. E. Jones, and M. J. Anderson. 1983. Characterization of the genome of the agent of erythrocyte aplasia permits its classification as a human parvovirus. J Gen Virol 64 (Pt 11). 2527-2532.

Summers, M. D., and G. E. Smith. 1978. Baculovirus structural polypeptides. Virology 84. 390-402.

Summers, M. D., and G. E. Smith. 1987. A manual of methods for baculovirus vectors and insect cell culture procedures. Texas Agricultural Experiment Station Bulletin., Vol. No. 1555.,

Takahashi, Y., C. Murai, S. Shibata, Y. Munakata, T. Ishii, K. Ishii, T. Saitoh, T. Sawai, K. Sugamura, and T. Sasaki. 1998. Human parvovirus B19 as a causative agent for rheumatoid arthritis. Proc Natl Acad Sci U S A 95. 8227-8232.

Tami, C., M. Farber, E. L. Palma, and O. Taboga. 2000. Presentation of antigenic sites from foot-and-mouth disease virus on the surface of baculovirus and in the membrane of infected cells. Arch Virol 145. 1815-1828.

Tattersall, P., P. J. Cawte, A. J. Shatkin, and D. C. Ward. 1976. Three structural polypeptides coded for by minite virus of mice, a parvovirus. J Virol 20. 273-289.

Tattersall, P., A. J. Shatkin, and D. C. Ward. 1977. Sequence homology between the structural polypeptides of minute virus of mice. J Mol Biol 111. 375-394.

Tjernberg, L. O., A. Pramanik, S. Bjorling, P. Thyberg, J. Thyberg, C. Nordstedt, K. D. Berndt, L. Terenius, and R. Rigler. 1999. Amyloid beta-peptide polymerization studied using fluorescence correlation spectroscopy. Chem Biol 6. 53-62.

Tratschin, J. D., J. Tal, and B. J. Carter. 1986. Negative and positive regulation in trans of gene expression from adeno-associated virus vectors in mammalian cells by a viral rep gene product. Mol Cell Biol 6. 2884-2894.

Trepagnier, E. H., C. Jarzynski, F. Ritort, G. E. Crooks, C. J. Bustamante, and J. Liphardt. 2004. Experimental test of Hatano and Sasa's nonequilibrium steady-state equality. Proc Natl Acad Sci U S A 101. 15038-15041.

Trier, U., Z. Olah, B. Kleuser, and M. Schafer-Korting. 1999. Fusion of the binding domain of Raf-1 kinase with green fluorescent protein for activated Ras detection by fluorescence correlation spectroscopy. Pharmazie 54. 263-268.

Truyen, U., M. Agbandje, and C. R. Parrish. 1994. Characterization of the feline host range and a specific epitope of feline panleukopenia virus. Virology 200. 494-503.

Tsao, J., M. S. Chapman, M. Agbandje, W. Keller, K. Smith, H. Wu, M. Luo, T. J. Smith, M. G. Rossmann, and R. W. Compans. 1991. The three-dimensional structure of canine parvovirus and its functional implications. Science 251. 1456-1564.

Vafaie, J., and R. A. Schwartz. 2004. Parvovirus B19 infections. Int J Dermatol 43. 747-749.

van den Berg, P. A. W., J. Widengren, M. A. Hink, R. Rigler, and A. J. W. G. Visser. 2001. Fluorescence correlation spectroscopy of flavins and flavoenzymes: photochemical and photophysical aspects. Spectrochim Acta A 57. 2135-2144.

Vercammen, J., G. Maertens, M. Gerard, E. De Clercq, Z. Debyser, and Y. Engelborghs. 2002. DNA-induced polymerization of HIV-1 integrase

analyzed with fluorescence fluctuation spectroscopy. J Biol Chem 277. 38045-38052.

Vihinen-Ranta, M., S. Suikkanen, and C. R. Parrish. 2004. Pathways of cell infection by parvoviruses and adeno-associated viruses. J Virol 78. 6709-6714.

Vihinen-Ranta, M., D. Wang, W. S. Weichert, and C. R. Parrish. 2002. The VP1 N-Terminal Sequence of Canine Parvovirus Affects Nuclear Transport of Capsids and Efficient Cell Infection. J Virol 76. 1884-1891.

Volkman, L. E. 1997. Nucleopolyhedrovirus interactions with their insect hosts. Adv Virus Res 48. 313-348.

Vukojevic, V., T. Yakovleva, L. Terenius, A. Pramanik, and G. Bakalkin. 2004. Denaturation of dsDNA by p53: fluorescence correlation spectroscopy study. Biochem Biophys Res Commun 316. 1150-1155.

Wachsmuth, M., W. Waldeck, and J. Langowski. 2000. Anomalous diffusion of fluorescent probes inside living cell nuclei investigated by spatially-resolved fluorescence correlation spectroscopy. J Mol Biol 298. 677-689.

Washburn, J. O., E. H. Lyons, E. J. Haas-Stapleton, and L. E. Volkman. 1999. Multiple nucleocapsid packaging of Autographa californica nucleopolyhedrovirus accelerates the onset of systemic infection in Trichoplusia ni. J Virol 73. 411-416.

Weichert, W. S., J. S. Parker, A. T. Wahid, S. F. Chang, E. Meier, and C. R. Parrish. 1998. Assaying for structural variation in the parvovirus capsid and its role in infection. Virology 250. 106-117.

Weiner, O. H., M. Alt, R. Durr, A. A. Noegel, and W. H. Caselmann. 2000. Rapid and reproducible quantification of hepatitis C virus cDNA by fluorescence correlation spectroscopy. Digestion 61. 84-89.

Widengren, J., U. Mets, and R. Rigler. 1999. Photodynamic properties of green fluorescent proteins investigated by fluorescence correlation spectroscopy. Chem Phys 250. 171-186.

Widengren, J., Ü. Mets, and R. Rigler. 1995. Fluorescence Correlation Spectroscopy of Triplet States in Solution: A Theoretical and Experimental Study. J Phys Chem 99. 13368-13379.

Widengren, J., and R. Rigler. 1997. An alternative way of monitoring ion concentrations and their regulation using fluorescence correlation spectoscopy. J Fluoresc 7. 211-213.

Widengren, J., and R. Rigler. 1998. Fluorescence correlation spectroscopy as a tool to investigate chemical reactions in solutions and on cell surfaces. Cell Mol Biol 44. 857-879.

Widengren, J., R. Rigler, and Ü. Mets. 1994. Triplet-State Monitoring by Fluorescence Correlation Spectroscopy. J Fluoresc 4. 255-258.

Wikoff, W. R., G. Wang, C. R. Parrish, R. H. Cheng, M. L. Strassheim, T. S. Baker, and M. G. Rossmann. 1994. The structure of a neutralized virus: canine parvovirus complexed with neutralizing antibody fragment. Structure 2. 595-607.

Wilk, A., J. Gapinski, and A. Patkowski. 2004. Self-Diffusion in solutions of a 20 base pair oligonucleotide: Effects of concentration and ionic strength. J Chem Phys 121. 10794-10802.

Wu, H., and M. G. Rossmann. 1993. The canine parvovirus empty capsid structure. J Mol Biol 233. 231-244.

Xia, S., S. Kjaer, K. Zheng, P. S. Hu, L. Bai, J. Y. Jia, R. Rigler, A. Pramanik, T. Xu, T. Hokfelt, and Z. Q. Xu. 2004. Visualization of a functionally enhanced GFP-tagged galanin R2 receptor in PC12 cells: constitutive and ligand-induced internalization. Proc Natl Acad Sci U S A 101. 15207-15212.

Xie, Q., and M. S. Chapman. 1996. Canine parvovirus capsid structure, analyzed at 2.9 A resolution. J Mol Biol 264. 497-520.

Yakovleva, T., A. Pramanik, T. Kawasaki, K. Tan-No, I. Gileva, H. Lindegren, U. Langel, T. J. Ekstrom, R. Rigler, L. Terenius, and G. Bakalkin. 2001. p53 Latency. C-terminal domain prevents binding of p53 core to target but not to nonspecific DNA sequences. J Biol Chem 276. 15650-15658.

Yakovleva, T., A. Pramanik, L. Terenius, T. J. Ekstrom, and G. Bakalkin. 2002. p53 latency-out of the blind alley. Trends Biochem Sci 27. 612-618.

Yoshida, N., M. Kinjo, and M. Tamura. 2001. Microenvironment of endosomal aqueous phase investigated by the mobility of microparticles using fluorescence correlation spectroscopy. Biochem Biophys Res Commun 280. 312-318.

Young, N. S. 1995. B19 parvovirus. Baillieres Clin Haematol 8. 25-56.

Yuan, W., and C. R. Parrish. 2001. Canine parvovirus capsid assembly and differences in mammalian and insect cells. Virology 279. 546-557.

Zadori, Z., J. Szelei, M. C. Lacoste, Y. Li, S. Gariepy, P. Raymond, M. Allaire, I. R. Nabi, and P. Tijssen. 2001. A viral phospholipase A2 is required for parvovirus infectivity. Dev Cell 1. 291-302.

Zeiss, C. 2001. *Application Manual LSM 510 - ConfoCor 2*, D-07740 Jena.